

Validation of ACE-FTS v2.2 measurements of HCl, HF, CCl₃F and CCl₂F₂ using space-, balloon- and ground-based instrument observations

E. Mahieu¹, P. Duchatelet¹, P. Demoulin¹, K. A. Walker^{2,3}, E. Dupuy³, L. Froidevaux⁴, C. Randall⁵, V. Catoire⁶, K. Strong², C. D. Boone³, P. F. Bernath⁷, J.-F. Blavier⁴, T. Blumenstock⁸, M. Coffey⁹, M. De Mazière¹⁰, D. Griffith¹¹, J. Hannigan⁹, F. Hase⁸, N. Jones¹¹, K. W. Jucks¹², A. Kagawa¹³, Y. Kasai¹³, Y. Mebarki⁶, S. Mikuteit⁸, R. Nassar¹⁴, J. Notholt¹⁵, C. P. Rinsland¹⁶, C. Robert⁶, O. Schrems¹⁷, C. Senten¹⁰, D. Smale¹⁸, J. Taylor², C. Tétard¹⁹, G. C. Toon⁴, T. Warneke¹⁵, S. W. Wood¹⁸, R. Zander¹, and C. Servais¹

¹Groupe Infra-Rouge de Physique Atmosphérique et Solaire (GIRPAS), Institute of Astrophysics and Geophysics, University of Liège, Liège, Belgium

²Department of Physics, University of Toronto, 60 St. George Street, Toronto, Ontario, M5S 1A7, Canada

³Department of Chemistry, University of Waterloo, 200 University Avenue West, Waterloo, Ontario, N2L 3G1, Canada

⁴Jet Propulsion Laboratory, California Institute of Technology, Pasadena, CA, USA

⁵University of Colorado, CO, USA

⁶Lab. de Physique et Chimie de l'Environnement, CNRS – Univ. d'Orléans (UMR 6115), 45071 Orléans Cedex 2, France

⁷Department of Chemistry, University of York, Heslington, York, YO10 5DD, UK

⁸Institute for Meteorology and Climate Research (IMK), Forschungszentrum Karlsruhe and University of Karlsruhe, Karlsruhe, Germany

⁹National Center for Atmospheric Research, CO, USA

¹⁰Belgian Institute for Space Aeronomy, Brussels, Belgium

¹¹University of Wollongong, Australia

¹²Harvard-Smithsonian Center for Astrophysics, Cambridge, MA, USA

¹³National Institute of Communications and Information Technology, 4-2-1 Nukui-kita, Koganei, Tokyo 184-8795, Japan

¹⁴Harvard University, Cambridge, MA, USA

¹⁵Institute of Environmental Physics, University of Bremen, Germany

¹⁶Langley Research Center, VA, USA

¹⁷Alfred Wegener Institute for Polar and Marine Research, Bremerhaven, Germany

¹⁸National Institute of Water and Atmospheric Research Ltd, Lauder, Central Otago, New Zealand

¹⁹Laboratoire d'Optique Atmosphérique, Université des sciences et technologies de Lille (UMR 8518), 59655 Villeneuve d'Ascq, France

Received: 4 December 2007 – Published in Atmos. Chem. Phys. Discuss.: 18 February 2008

Revised: 30 June 2008 – Accepted: 9 September 2008 – Published: 27 October 2008

Abstract. Hydrogen chloride (HCl) and hydrogen fluoride (HF) are respectively the main chlorine and fluorine reservoirs in the Earth's stratosphere. Their buildup resulted from the intensive use of man-made halogenated source gases, in particular CFC-11 (CCl₃F) and CFC-12 (CCl₂F₂), during the second half of the 20th century. It is important to

continue monitoring the evolution of these source gases and reservoirs, in support of the Montreal Protocol and also indirectly of the Kyoto Protocol. The Atmospheric Chemistry Experiment Fourier Transform Spectrometer (ACE-FTS) is a space-based instrument that has been performing regular solar occultation measurements of over 30 atmospheric gases since early 2004. In this validation paper, the HCl, HF, CFC-11 and CFC-12 version 2.2 profile data products retrieved from ACE-FTS measurements are evaluated. Volume mixing



Correspondence to: E. Mahieu
(emmanuel.mahieu@ulg.ac.be)

ratio profiles have been compared to observations made from space by MLS and HALOE, and from stratospheric balloons by SPIRALE, FIRS-2 and Mark-IV. Partial columns derived from the ACE-FTS data were also compared to column measurements from ground-based Fourier transform instruments operated at 12 sites. ACE-FTS data recorded from March 2004 to August 2007 have been used for the comparisons. These data are representative of a variety of atmospheric and chemical situations, with sounded air masses extending from the winter vortex to summer sub-tropical conditions. Typically, the ACE-FTS products are available in the 10–50 km altitude range for HCl and HF, and in the 7–20 and 7–25 km ranges for CFC-11 and -12, respectively. For both reservoirs, comparison results indicate an agreement generally better than 5–10% above 20 km altitude, when accounting for the known offset affecting HALOE measurements of HCl and HF. Larger positive differences are however found for comparisons with single profiles from FIRS-2 and SPIRALE. For CFCs, the few coincident measurements available suggest that the differences probably remain within $\pm 20\%$.

1 Introduction

Under unperturbed atmospheric conditions, hydrogen chloride (HCl) and hydrogen fluoride (HF) are the two most abundant halogenated species of the inorganic chlorine and fluorine families (respectively denoted Cl_y and F_y; see e.g. Prinn et al. (1999)) in the stratosphere. Since the 1970s, their atmospheric concentrations have significantly increased, followed by a recent slowing down in their accumulation, and even a decrease for HCl (Mahieu et al., 2004; Froidevaux et al., 2006b). Indeed, the respective HCl and HF mean upper stratospheric concentrations have risen from 2500 and 760 pptv in the mid-1980s to 3800 and 1800 pptv in the first years of the new millennium (e.g., Zander et al., 1992; Gunson et al., 1994; Nassar et al., 2006a, b). These increases are due to the extensive use of man-made chlorofluorocarbons (CFCs), further augmented, and then replaced, with substitutes such as hydrochlorofluorocarbons (HCFCs). Among these source gases, the main contributors are CCl₂F₂ (CFC-12) and CCl₃F (CFC-11), with current mean tropospheric concentrations of 540 and 250 pptv, respectively (WMO Report Nr. 50, 2007). Transport of these long-lived compounds to the stratosphere leads to their photodissociation, with release of chlorine and fluorine atoms (e.g., Kaye et al., 1991). Rapid recombination of these atoms with hydrogenated compounds (e.g., CH₄, H₂) respectively produces HCl and HF, the two reservoir species of interest here. However, before the formation of HCl, Cl can be involved in the ClO_x catalytic cycle which contributes to ozone depletion (e.g., Molina and Rowland, 1974).

HF is a remarkably stable species in the stratosphere (e.g., Stolarski and Rundel, 1975), making it an ideal tracer of

transport and dynamics in this atmospheric region (Chipperfield et al., 1997). Conversely, HCl can be activated under specific conditions occurring mainly in the stratospheric polar atmosphere and in wintertime, with the production of active chlorine species (e.g., ClO) which are able to destroy ozone. This reactivation occurs through various heterogeneous reactions taking place on Polar Stratospheric Clouds (PSCs), at temperatures below 200 K (e.g. Solomon et al., 1999; WMO Report Nr. 50, 2007, and references therein).

Even before the unambiguous confirmation of the significant role of anthropogenic chlorine in the destruction of the Earth's protective ozone layer, monitoring networks such as the AGAGE (Advanced Global Atmospheric Gases Experiment) and NOAA/ESRL (National Oceanic and Atmospheric Administration – Earth System Research Laboratory) have been measuring increases in a large number of source gases, including all major long-lived CFCs and HCFCs, by in situ surface sampling (e.g., O'Doherty et al., 2004; Montzka et al., 1999, and references therein). These increasing tropospheric loadings were at the heart of the alarming threat to ozone suggested by Molina and Rowland (1974). This theory was soon supported by the first detections in the stratosphere of HF (Zander et al., 1975), of HCl (Farmer et al., 1976; Ackerman et al., 1976), and of CFC-11 and -12 (Murcray et al., 1975).

The ATMOS (Atmospheric Trace MOlecule Spectroscopy, <http://remus.jpl.nasa.gov/atmos>) Fourier Transform InfraRed (FTIR) instrument was one of the pioneering space-based experiments that measured the vertical distributions of nearly 30 atmospheric gases, during four shuttle flights that took place from 1985 to 1994 (Gunson et al., 1996). Among the many results of ATMOS, chlorine and fluorine budgets were evaluated using Northern latitude measurements of halogenated sources and reservoirs, supplemented by balloon and model data for a few missing species (Raper et al., 1987; Zander et al., 1987, 1992 and 1996). HALOE (HALOgen Occultation Experiment; Russell et al. (1993)) has contributed over the longer term, recording regular, global occultation measurements of HCl and HF between September 1991 and November 2005. The HALOE data set has been used to derive the first global distributions and decadal trends of HCl and HF from space (e.g., Anderson et al., 2000; WMO Report Nr. 50, 2007). These stratospheric species have also been remotely monitored from the ground, using FTIRs. Data sets now spanning more than 30 years are available from the Jungfraujoch station, allowing long-term trends in HCl and HF to be characterized (e.g., Rinsland et al., 2002; Mahieu et al., 2004; WMO Report Nr. 50, 2007). Other sites equipped with FTIRs and affiliated with the Network for the Detection of Atmospheric Composition Change (NDACC, previously NDSC, <http://www.ndacc.org>), have also contributed to this effort. Observations from nine sites spread from Northern high- to Southern mid-latitudes have detected the leveling-off of HCl, which peaked around the mid-1990s (Rinsland et al.,

2003). In parallel, experiments using balloon-borne instruments, often focusing on polar vortex chemistry in the low stratosphere, have provided complementary information for both the source and reservoir species (e.g., Sen et al., 1998).

Among the space-borne instruments currently performing observations of these species, MLS (Microwave Limb Sounder) onboard Aura has collected HCl data over the last three years and is still in operation (Froidevaux et al., 2006b). ACE-FTS (Atmospheric Chemistry Experiment Fourier Transform Spectrometer), onboard the Canadian SCISAT satellite, is also still fully operational after more than four years in space and is the only instrument presently in orbit which measures HF. Previous work using ACE-FTS observations has included studies of the global inventories and partitioning of stratospheric chlorine and fluorine, using the version 2.2 (v2.2) data set (Nassar et al., 2006a, b).

Although the HCl and HF version 1.0 (v1.0) data products were targets of initial comparisons (e.g., McHugh et al., 2005; Mahieu et al., 2005), the more extensive v2.2 database still requires validation. Therefore, the present study aims at investigating the consistency and reliability of the ACE v2.2 HCl, HF, CFC-11 and -12 level 2 products, prior to their official release to the scientific community. For this purpose, the present manuscript has been organized into several sections. Section 2 briefly describes the ACE-FTS instrument and measurements, as well as the strategy adopted in the retrieval processes. Section 3 gives an overview of the correlative data sets and instruments involved, as well as details on selected data filtering and collocation criteria. Section 4 deals with intercomparison results, on a per-molecule and per-instrument basis. Finally, conclusions are given in Sect. 5.

2 The ACE-FTS measurements of HCl, HF, CFC-11 and -12

The ACE-FTS instrument was launched onboard the SCISAT satellite on 12 August 2003. A low altitude (650 km) high inclination (74°) circular orbit was selected in order to allow for coverage of polar to tropical regions, in agreement with the mission's objectives (Bernath et al., 2005). The platform also carries a spectrophotometer (MAESTRO – Measurement of Aerosol Extinction in the Stratosphere and Troposphere Retrieved by Occultation, (McElroy et al., 2007)) as well as two filtered solar imagers (ACE-imagers, Gilbert et al., 2007). The ACE-FTS instrument achieves a maximum spectral resolution of 0.02 cm⁻¹ in the broad 750–4400 cm⁻¹ spectral interval (2.2 to 13 micrometers). The initial requirement for the S/N of the instrument was 100 over the whole spectral range. Over most of the interval, this has been exceeded by a factor 2 to 3 (Châteauneuf et al., 2004). Since the beginning of routine operations on 21 February 2004, this instrument has recorded up to 15 sunrise (sr) and sunset (ss) oc-

cultations per day (about every 90 min); successive infrared (IR) solar spectra are collected from 150 km altitude down to the cloud tops, with a vertical resolution of about 3–4 km, corresponding to 1.25 mrad field of view of ACE-FTS. As a result of the 2 s needed to record an interferogram and of the orbital beta angle, the vertical spacing of the measurements varies between 1.5 and 6 km (without including the effects of atmospheric refraction).

Analyses of ACE-FTS spectra (level 1 data) are performed at the University of Waterloo (Ontario, Canada). The algorithm is thoroughly described by Boone et al. (2005). In a first step, temperature and pressure are retrieved using CO₂ spectral lines, assuming a realistic profile. Subsequent retrievals of target species combine the information from several microwindows that are carefully selected to minimize the impact of interfering gases in the altitude range of interest, i.e., generally from the lower mesosphere to the upper troposphere. Inversion of a series of successive spectra recorded during a solar occultation event produces volume mixing ratio (vmr) profiles of the target gases, on the measured altitude grid. These profiles are also interpolated onto a standard altitude grid, consisting of 150 levels of 1 km thickness, which are considered to be homogeneous in terms of pressure, temperature and vmr of the various gases.

While profiles of more than 30 species are now retrieved from the ACE-FTS measurements, a group of primary (“baseline”) data products have been selected by the ACE Science Team as the focus of this validation exercise. These include O₃, CH₄, H₂O, NO, NO₂, ClONO₂, HNO₃, N₂O, N₂O₅, HCl, CCl₃F, CCl₂F₂, HF, CO, aerosols, temperature and pressure.

ACE-FTS retrievals considered here have been performed using the standard edition of the HITRAN-2004 line parameter and cross section compilation (Rothman et al., 2005). The microwindows used in the HCl, HF, CFC-11 and CFC-12 retrievals are listed in Table 1, together with the main interfering species and the altitude range in which each microwindow is used. Several spectral intervals encompassing discrete lines are simultaneously used to retrieve HCl and HF vmrs.

For CFCs, broad spectral features are used to retrieve their vertical distributions, typically between the tangent height of 10 and 25 km.

Version 2.2 retrievals are identical to v1.0 settings, except for HCl. In the new approach, microwindows encompassing absorption lines of the H³⁷Cl isotopologue have been included, 22 spectral intervals are used instead of the 13 used previously. It should be noted that, to date, no formal complete error budget has been produced for the ACE-FTS v2.2 retrievals.

Table 1. Microwindows used for the ACE-FTS retrievals of HCl, HF, CFC-11 and -12.

Central Freq (cm ⁻¹)	Width (cm ⁻¹)	Alt.Range (km)	Remarks
HCl			
2701.26	0.3	8–36	Interfering molecules for HCl windows: O ₃ below 40 km CH ₄ below 50 km
2703.03	0.3	35–47	
2727.77	0.4	8–45	
2751.97	0.3	47–55	
2775.75	0.3	40–55	
2798.95	0.35	51–57	
2819.48	0.3	20–54	
2821.47	0.3	18–57	
2841.63	0.4	20–50	
2843.67	0.3	15–57	
2865.16	0.26	38–57	
2906.30	0.3	45–57	
2923.57	0.5	20–48	
2923.73	0.3	44–50	
2925.90	0.3	17–57	
2942.67	0.4	15–54	
2944.95	0.3	10–57	
2961.00	0.4	25–48	
2963.11	0.5	8–57	
2981.00	0.5	40–57	
2995.88	0.3	45–51	
2998.14	0.3	52–57	
HF			
1815.78 ^a	0.3	25–35	Interfering molecules for HF windows: H ₂ O below 30 km O ₃ below 35 km N ₂ O below 25 km CH ₄ below 23 km
1987.34 ^b	0.3	10–30	
2010.70 ^a	0.3	10–25	
2667.47 ^c	0.35	10–23	
2814.40 ^d	0.3	10–25	
3788.33	0.4	10–44	
3833.71	0.4	18–48	
3877.75	0.35	10–50	
3920.39	0.3	27–50	
4001.03	0.3	10–50	
4038.87	0.45	10–50	
4109.94	0.35	25–46	
4142.97	0.4	15–40	
CCl₃F (CFC-11)			
842.50	25	5–22	CO ₂ below 22 km HNO ₃ below 22 km H ₂ O below 22 km O ₃ below 22 km
CCl₂F₂(CFC-12)			
922	4	6–28	O ₃ below 25 km
1161	1.2	12–25	N ₂ O below 25 km

^aIncluded to improve results for interferer O₃^bIncluded to improve results for interferer H₂O^cIncluded to improve results for interferer CH₄^dIncluded to improve results for interferer N₂O

3 Correlative data sets

In the following sub-sections, all instruments and corresponding measurements will be briefly described; specific methodology for comparison, if any, as well as the criteria used for selecting the coincidences will also be provided.

3.1 MLS v2.2 measurements of HCl

Continuous (day and night) global measurements of HCl have been provided since August 2004 by MLS onboard the Aura satellite. MLS measures thermal emission lines from trace gases at millimeter and sub-millimeter wavelengths, as discussed by Waters et al. (2006). Validation of the MLS HCl version 2.2 (v2.2) data has been described recently by Froidevaux et al. (2008). This data version has been used since March 2007. The reprocessing of the MLS data is still ongoing. The single profile precision of MLS HCl is 0.5 ppbv or less in the stratosphere, and the HCl accuracy estimate is about 0.2 ppbv. The recommended altitude range for MLS HCl profiles is from 100 to 0.15 hPa; the data can be used down to 150 hPa at high latitudes, although a high MLS bias is observed at low to mid-latitudes versus aircraft in situ data at this pressure level (Froidevaux et al., 2008). More details regarding the MLS experiment and the HCl data screening are provided in the above references; per these references, we follow the MLS flags that screen out a small percentage of profiles with bad “Status”, and poor “Quality” (from radiance fits) or “Convergence” (retrieval issue). In this work, the comparisons of coincident profiles between MLS and ACE-FTS include 4731 ACE-FTS occultations between 84° N and 84° S latitude. The number of MLS v2.2 reprocessed days available at the time of writing for 2004, 2005, and 2006 were 28, 179 and 154, respectively. For 2007, the comparisons include data from MLS and ACE-FTS until the end of August, although no MLS HCl data were obtained from 15 July through 9 August, due to a temporary instrument anomaly. The coincidence criteria used here are the same as those used in the analyses by Froidevaux et al. (2008). For each ACE-FTS profile, the closest MLS profile (on the same day) within ±2 degrees of latitude and ±8 degrees of longitude is selected. The ACE-FTS profiles are interpolated (linearly versus log of pressure) onto the MLS retrieval grid, using the retrieved pressures from the ACE-FTS data.

3.2 HALOE v19 measurements of HCl and HF

The HALOE instrument was in operation onboard the UARS platform (Upper Atmospheric Research Satellite; Reber et al. (1993)) for 14 years, from September 1991 to November 2005, when the mission was ended. Therefore, it operated throughout most of the first two years of the ACE mission operations phase. Given the UARS orbital inclination of 57° and the satellite altitude (close to 600 km), HALOE was able to sample the Earth’s atmosphere almost globally (from

about 80° N to 80° S), in solar occultation mode, from the lower mesosphere to the upper troposphere. Eight IR channels allow the measurements of several trace gases (e.g., O₃, CH₄, H₂O) with a vertical resolution of ~2 km. HCl and HF vertical distributions are among the available data products.

Earlier version 17 (v17) HALOE HCl data were found to agree with correlative measurements to within about 10–20% in the stratosphere, with a possible low bias (Russell et al., 1996a). Comparisons between version 19 (v19) HALOE and v1.0 ACE-FTS data were described by McHugh et al. (2005), who found that ACE-FTS HCl was within ±10% of HALOE below 20 km, and 10–20% higher than HALOE from 20 to 48 km. In a recent paper, Lary et al. (2007) have compared several space-based measurements of HCl, by ACE-FTS, ATMOS, HALOE and MLS, obtained between 1991 and 2006, using a neural network. They further confirmed the low bias of HALOE with respect to all other instruments.

For HF, v17 HALOE data were found to agree with correlative balloon measurements to better than 7% from 5 to 50 hPa (i.e., between about 20 and 35 km) (Russell et al., 1996b), but had a similar 10–20% low bias with respect to ATMOS as was observed for HCl (Russell et al., 1996a). Comparisons between v19 HALOE and v1.0 ACE-FTS data were also performed by McHugh et al. (2005), who found that ACE-FTS HF was about 10–20% higher than HALOE from 15 to 45 km.

The latest version (v19; available from e.g. <http://badc.nerc.ac.uk/data/haloe>) data release has been used in the present statistical analyses, for both HCl and HF.

The HALOE and ACE-FTS data sets were searched for coincident profile measurements, defined as occurring within 2 hours in time and 500 km in geographic distance. A total of 36 coincidences were found; 5 corresponding to sunrise occultations and 31 to sunset occultations. Relaxing the time criterion to one day did not result in any new coincidences. Twenty nine coincidences occurred from 4 to 10 July 2004 (average latitude 66° N) and two on 15 August 2005 (average latitude 49° S); the five sunrise coincidences occurred on 6 and 7 September 2004 (5 coincidences, average latitude 60° N). Thus most of the comparisons correspond to polar summer conditions in the Northern Hemisphere.

3.3 SPIRALE measurements of HCl

SPIRALE (SPectroscopie Infra-Rouge d'Absorption par Lasers Embarqués) is a balloon-borne instrument operated by LPCE (Laboratoire de Physique et de Chimie de l'Environnement, CNRS – Université d'Orléans) and routinely used at all latitudes, in particular as part of European validation campaigns for the Odin and Envisat missions. This six tunable diode laser absorption spectrometer (TDLAS) has been previously described in detail (Moreau et al., 2005). In brief, it can perform simultaneous *in situ* measurements of about ten chemical species from about 10 to 35 km height, with a high frequency sampling (~1 Hz), thus

enabling a vertical resolution of a few meters depending on the ascent rate of the balloon. The diode lasers emit in the mid-infrared domain (from 3 to 8 μm) with beams injected into a multipass Herriott cell located under the gondola and exposed to ambient air. The cell (3.5 m long) is deployed during the ascent when pressure is lower than 300 hPa. The multiple reflections obtained between the two cell mirrors give a total optical path of 430.78 m. Species concentrations are retrieved from direct infrared absorption, by adjusting synthetic spectra calculated using the HITRAN 2004 database (Rothman et al., 2005) to match the observation. Specifically, the ro-vibrational line at 2925.8967 cm⁻¹ was used for HCl. Measurements of pressure (from two calibrated and temperature-regulated capacitance manometers) and temperature (from two probes made of resistive platinum wire) aboard the gondola allow the species concentrations to be converted to vmrs.

Uncertainties in these pressure and temperature parameters have been evaluated to be negligible relative to the other uncertainties discussed below. The global uncertainties on the vmrs have been assessed by taking into account the random errors and the systematic errors, and combining them as the square root of their quadratic sum. The two important sources of random error are the fluctuations of the laser background emission signal and the signal-to-noise ratio. At lower altitudes (below 16 km), these are the main contributions. Systematic errors originate essentially from the laser line width (an intrinsic characteristic of the diode laser), which contributes more at lower pressure (higher altitudes) than at higher pressures. The impact of the spectroscopic parameter uncertainties (essentially the molecular line strength and pressure broadening coefficients) on the vmr retrievals is almost negligible. After quadratic combination, the random and systematic errors result in total uncertainties of 20% below 16 km altitude, decreasing to 13% at 23 km and to a constant value of 7% above 23 km.

The SPIRALE measurements occurred on 20 January 2006 between 17:36 UT and 19:47 UT. An HCl vertical profile was obtained during ascent, between 11.3 and 27.3 km height. The measurement position remained rather constant with a mean location of the balloon at (67.6±0.2)° N and (21.55±0.20)° E. The comparison is made with the ACE-FTS sunrise occultation (sr13151) that occurred 13 h later (on 21 January 2006 at 08:00 UT) and was located at 64.28° N–21.56° E, i.e., 413 km distant from the mean SPIRALE position.

3.4 FIRS-2 measurements of HCl, HF, CFC-11 and CFC-12

The Far-InfraRed Spectrometer (FIRS)-2 is a thermal emission FTIR spectrometer designed and built at the Smithsonian Astrophysical Observatory. The balloon-borne limb-sounding observations provide high-resolution (0.004 cm⁻¹) spectra in the wavelength range 7–120 μm (80–1400 cm⁻¹)

(Johnson et al., 1995), at altitude levels from the tropopause to the balloon float altitude (typically 38 km). The retrievals are conducted in a two-step process. First, the atmospheric pressure and temperature profiles are retrieved from observations of CO₂ spectral lines around 15 μm . Then, vertical profiles of atmospheric trace constituents are retrieved using a nonlinear Levenberg-Marquardt least-squares algorithm (Johnson et al., 1995). Vertical vmr profiles are routinely produced for ~ 30 molecular species including HCl, HF, CFC-11 and CFC-12. In particular, FIRS-2 retrieves HCl and HF using 11 and 3 rotational lines, respectively. CFC-11 and CFC-12 are retrieved using the same bands as ACE-FTS (see relevant part of Table 1).

Uncertainty estimates for FIRS-2 contain random retrieval error from spectral noise and systematic components from errors in atmospheric temperature and pointing angle (Jucks et al., 2002; Johnson et al., 1995). The HCl retrievals yield total errors decreasing with increasing altitude from 55% at 12 km to 9% at 22 km and smaller than 7% above 22 km. The HF errors are small ($<10\%$) from 16 to 31 km, with larger values ($\sim 60\%$) below this range. For CFC-11, the total error for the profile used in this study increases with increasing altitude, from 24% at 12 km to 90% around 20 km. Lastly, the error values for CFC-12 increase from 55 to 100% over the same altitude range.

Measurements from FIRS-2 have been used previously in conjunction with other balloon-borne instruments to validate observations of the v17 HCl data product from HALOE (Russell et al., 1996a). HALOE showed a positive bias with respect to FIRS-2 decreasing with altitude, with mean differences ranging from +19% at ~ 17 km (100 hPa) to +9% at ~ 31 km (5 hPa) (Russell et al., 1996a). A comparison of the HALOE v17 HF retrievals with data from the same balloon flights, presented in the companion paper of Russell et al. (1996b), yielded agreement within $\pm 7\%$ in the altitude range ~ 21 –31 km (50–5 hPa) with much larger differences at the lowermost comparison levels (-53% at 100 hPa or 17 km) (Russell et al., 1996b).

The FIRS-2 profiles were acquired on 24 January 2007 at 10:11 UT (68° N, 22° E). The coincident ACE-FTS profiles were obtained at sunrise on 23 January 2007 at 08:25 UT (occultation sr18561, 64.7° N, 15.0° E; distance: ~ 481 km). The low float altitude (~ 28 km) of the balloon for this particular flight limits the vertical range of the comparison to 31 km. It should be noted that the precision for the CFCs was below normal for this specific FIRS-2 flight, given the short time at float altitude and very cold temperatures lowering the signal-to-noise ratio (S/N) in the wavelength region from which CFCs are retrieved. The FIRS-2 profiles, provided on a 1 km-spacing altitude grid, are interpolated onto the ACE-FTS altitude grid (1 km-spacing). The position of the FIRS-2 footprint was well inside the Arctic vortex, while the ACE-FTS footprint was near the edge of the vortex. As a result, atmospheric subsidence mismatches could possibly affect the comparisons. We have therefore looked at

the equivalence between altitude and potential temperature (θ), for both subsets. This has indicated that maximum vertical shifting resulting from the use of potential temperature would never exceed 0.9 km, for a θ of 340 K, around 12 km. Over the whole range spanning available measurements from both instruments, the mean computed shift is equal to 0.3 km. Hence, comparisons performed using either altitude or potential temperature shows very similar pattern for the absolute and relative differences. We have therefore decided to present all the comparisons between FIRS-2 and ACE-FTS against altitude, for consistency with all other investigations reported here.

3.5 Mark-IV measurements of HCl, HF, CFC-11 and -12

The Jet Propulsion Laboratory (JPL) Mark-IV (hereinafter MkIV) Interferometer (Toon, 1991) is an FTIR spectrometer designed for remote sensing of atmospheric composition and is optically very similar to the ATMOS instrument. It has been used for ground-based observations as well as balloon-borne measurements since 1985. When flown as part of a high-altitude balloon payload, it provides solar occultation measurements in the spectral range 1.77–15.4 μm (650 – 5650 cm^{-1}), with high signal-to-noise ratio and high resolution (0.01 cm^{-1}).

The retrieval altitude range generally extends from the cloud tops (5–10 km) to the float altitude (typically 38 km), with a vertical spacing of 0.9–3 km (depending on latitude and altitude) and a circular field-of-view of 3.6 mrad, yielding a vertical resolution of ~ 1.7 km for a 20 km tangent height (Toon et al., 1999).

The retrievals are conducted in two distinct steps. Firstly, slant column abundances are retrieved from the spectra using non-linear least squares fitting. Secondly, the matrix equation relating these measured slant columns to the unknown vmr profiles and the calculated slant path distances is solved. This produces retrieved vmr vertical profiles for a large number of trace gas species including HCl, HF, CFC-11 and CFC-12 (Toon et al., 1999).

The uncertainty in the MkIV profiles is dominated by measurement noise and spectroscopic errors. Other error sources (such as temperature uncertainties or pointing error) can usually be neglected (Sen et al., 1998). The reported error for the HCl profiles used in the following analyses ranges from 3 to 10% above ~ 18 km. At lower altitudes, the error increases but remains smaller than 100% above ~ 15 km. The HF errors are also quite small ($<10\%$) from 20 to 38 km, with values rapidly increasing below this range (e.g., 50–70% at 17 km depending on the flight). The total error on the CFC-11 retrievals is within 20% below 25 km but, above this altitude, it becomes considerable. For CFC-12, the profiles used in this study have errors of 3 to 30% (typically 5%) over most of the altitude range (from 10 to 35 km) with larger values ($<100\%$) at the uppermost levels (Sen et al., 1998).

Table 2. Ground-based sites operating FTIR instruments involved in the present study.

Station	Latitude ° N	Longitude ° E	Altitude (m)	Related publication
Ny Ålesund	78.9	11.9	20	Notholt et al. (2000)
Thule	76.5	−68.7	30	Goldman et al. (1999)
Kiruna	67.8	20.4	419	Kopp et al. (2003)
Poker Flat	65.1	−147.4	610	Kagawa et al. (2007)
Bremen	53.1	8.8	50	Notholt et al. (2000)
Jungfraujoch	46.5	8	3580	Zander et al. (2008)
Toronto	43.7	−79.4	174	Wiacek et al. (2007)
Izaña	28.3	−16.5	2367	Schneider et al. (2005)
Reunion Island	−20.9	55.5	50	Senten et al. (2008)
Wollongong	−34.5	150.9	30	Paton-Walsh et al. (2005)
Lauder	−45	169.7	370	Griffith et al. (2003)
Arrival Heights	−77.8	166.7	200	Connor et al. (1998)

The quality of the MkIV observations was assessed through comparison with twelve in situ instruments embarked on the NASA ER-2 aircraft (Toon et al., 1999). The MkIV balloon and ER-2 aircraft flights occurred around Fairbanks (Alaska, USA) in 1997 as part of the Photochemistry of Ozone Loss in the Arctic Region In Summer (POLARIS) experiment. These comparisons included three of the four species considered here. Briefly, a very good agreement was found between MkIV and the in situ instrument, with differences for HCl and CFC-11 within $\pm 10\%$ and as low as $\pm 5\%$ for CFC-12. In all three cases, there was no apparent systematic bias between MkIV and the coincident measurements (Toon et al., 1999).

Prior to the present study, MkIV data have been used for satellite validation studies including several papers in the Journal of Geophysical Research special issue for UARS validation (J. Geophys. Res., 101(D6), 9539–10473, 1996) and the validation of ILAS data (Toon et al., 2002). More recently, the MkIV data have been compared with the MLS HCl product (Froidevaux et al., 2006a; Froidevaux et al., 2008). For HCl, MLS coincident profiles were compared with two MkIV observations around Ft. Sumner, New Mexico (34.4° N, 104.2° W) in September 2004 and showed good agreement – within the error bars – of 5 to 20% (Froidevaux et al., 2008).

For this work, we compare vmr profiles of HCl, HF, CFC-11 and CFC-12 retrieved from MkIV observations around Ft. Sumner, New Mexico, in September 2003, 2004 and 2005 with zonal averages of ACE-FTS data. There were no direct coincidences between ACE-FTS and the MkIV balloon flights, because ACE measurements around 35° N never occur during the late-September turnaround in stratospheric winds. The ACE-FTS profiles were thus selected within a 10° latitude band around Ft. Sumner between August and October in 2004, 2005 and 2006. At this time of the year, the atmospheric layers sounded by the instruments are suf-

ficiently stable to allow for meaningful qualitative comparisons. About 90 ACE-FTS profiles were available in a latitude bin of $\pm 5^\circ$ width centered at 34.4° N. These were averaged to provide a zonal mean profile.

3.6 Ground-based FTIR column measurements of HCl and HF

High-resolution IR solar spectra recorded under clear-sky conditions with ground-based FTIR (gb-FTIR) instruments have been analyzed to supply data for comparison with ACE-FTS v2.2 products. These observations have been recorded at 12 ground-based sites within the framework of the NDACC, with latitudes widely distributed among the two hemispheres. Table 2 lists the station coordinates. Most instruments are commercial Bruker interferometers, either IFS-125HR, -120HR or -120M, except at the Toronto and Wollongong stations where Bomem DA8 spectrometers are operated. These interferometers are equipped with mercury-cadmium-telluride (Hg-Cd-Te) and indium-antimonide (InSb) detectors, which allow coverage of the 650–1500 and 1650–4400 cm^{-1} spectral intervals, respectively. Spectral resolutions, defined as the inverse of the maximum optical path difference, range from 0.002 to 0.008 cm^{-1} .

All ground-based instruments involved here perform regular measurements encompassing the main IR absorption features of HCl, HF, CFC-11 and CFC-12. For the source gases however, the ground-based measurements are mostly sensitive to the tropospheric contribution of their absorptions, with poor or no vertical information available. These features are used to retrieve information on the atmospheric loadings of these two CFCs, and on their trends (e.g., Zander et al., 2005; Rinsland et al., 2005). Comparison with ACE-FTS measurements of the CFCs was not possible, as the ACE profiles are limited to the upper troposphere and lower stratosphere. Consequently, the FTIRs will contribute here to the validation of ACE-FTS v2.2 HCl and HF products, for which both

ground- and space-based viewing geometries provide reliable, compatible and comparable information, in the same altitude region of the atmosphere.

The retrievals have been performed using two algorithms. PROFFIT92 was used to analyze the Kiruna and Izana observations, SFIT2 (v3.8 or v3.9) in all other cases. Both codes are based on the Optimal Estimation Method (OEM) (Rodgers, 1976), they allow to retrieve information on the vertical distribution of most of the FTIR target gases, including HCl and HF. The two algorithms have been compared by Hase et al. (2004) for a series of tropospheric and stratospheric species and proved to be highly consistent, for profile and column retrievals; in particular, the agreement was better than 1% for both HCl and HF.

The OEM implemented in both algorithms helps to characterize the retrieved products, using the averaging kernel and related eigenvector formalism (e.g., Barret et al., 2003). Tools have been developed to perform these assessments and to evaluate the impact of the various fitting options, a priori inputs and assumptions made, on the information content.

Instead of using a single standardized retrieval strategy, approaches have been optimized by the FTIR data providers in order to generate the maximum information content for HCl and HF, taking into account specific observation conditions at each site (dryness, altitude, latitude, ...) as well as instrument performance characteristics, such as the typical signal-to-noise ratio achieved and the spectral resolution. Table 3 provides detailed information about the microwindows used simultaneously, the fitted interferences, the number of independent pieces of information available (given by the trace of the averaging kernel matrix) or Degrees Of Freedom for Signal (DOFS) and the altitude range of maximum sensitivity. Typical averaging kernels and eigenvectors corresponding to the adopted settings indicate that the retrievals of HCl and HF are mainly sensitive in the 12 to 35 km altitude range, with DOFS typically ranging from 1.4 to 3.8 for HCl and from 1.5 to 3.0 for HF (see Table 3). For Jungfraujoch, the first two eigenvalues (λ_1 and λ_2) are typically equal to 0.98 and 0.76, 0.98 and 0.66, respectively for HCl and HF, demonstrating that in both cases the impact of the a priori on the corresponding retrieved partial column is negligible, of the order of 2%. For most sites, additional information on the retrieval approaches adopted for HCl can be found in Appendix A of Rinsland et al. (2003). Relevant references are also provided in the last column of Table 2. It is worth noting that HITRAN-2004 line parameters (Rothman et al., 2005) were adopted in all cases, for target and interfering species, consistent with the ACE-FTS. Since the official release of HITRAN 2004 however, there has been several line parameter updates made available for gases interfering in the HCl or HF fitted intervals (e.g. H₂O, O₃). We have therefore performed retrievals using these various HITRAN updates to evaluate the impact of each linelists on the ground-based products. They have been found to be completely negligible. The impact of systematic uncertainties affecting the spectro-

scopic parameters of these species can therefore be neglected in the error budget.

On the basis of the Jungfraujoch retrievals, statistical error analyses complemented with estimates based on the perturbation method have indicated that the smoothing error is the main contribution to the error budget, followed by the measurement error and instrumental line shape uncertainties, independently evaluated with regular cell measurements. Once combined, the relative errors corresponding to stratospheric columns are on average about 2.6 and 3.2% for HCl and HF, respectively. Comparative and complementary error estimates have been generated from PROFFIT runs for typical Kiruna observations, including evaluation of the impact of random error sources such as zero level uncertainties, channeling and tilt, fitted interferences, temperature uncertainties, and effect of spectrum signal-to-noise. For both species, uncertainties in the temperature and zero level are the dominant error sources in this list. After quadratic combination, stratospheric column errors amount to $\sim 2.5\%$ for HCl, and $\sim 3.0\%$ for HF, i.e., commensurate with other estimates performed above.

Finally, HCl error budget evaluations performed in previous studies (e.g. Rinsland et al., 2003) further confirm the values quoted here, with a 3% random error associated with a single stratospheric column retrieval from Kitt Peak spectra.

As mentioned earlier, both PROFFIT and SFIT2 use the OEM formalism. This is particularly useful when performing comparisons between measurements obtained with significantly different vertical resolutions. Indeed, it has been shown by Rodgers and Connors (2003) that a fair comparison requires convolution of the high-vertical-resolution measurement (ACE-FTS here) with the averaging kernel of the low-vertical-resolution data (gb-FTIR) using the following equation:

$$x_S = x_a + A(x_{ACE} - x_a) \quad (1)$$

where x_S is the resulting smoothed profile, x_a is the FTIR a priori, x_{ACE} is the ACE-FTS retrieved vertical distribution and A is the FTIR averaging kernel.

Actual or typical averaging kernels have been used to perform these operations, after proper extrapolation of the ACE-FTS profile down to the altitude site, using x_a . For verification, extensions with other plausible vertical distributions were also performed for part of our dataset; we noted only marginal impact (on the order of a few tenths of a percent on average) on the partial columns computed on the basis of the smoothed ACE-FTS profiles.

For most sites, time and space criteria for coincidence with ACE-FTS measurements have been set to ± 24 h and 1000 km. However, the distance criterion was tightened to 500 km for Kiruna and Thule to minimize possible influence of the Polar vortex. For Reunion Island, it was relaxed to 1200 km to increase the number of coincidences, since there

Table 3. Information about retrieval strategies adopted at each ground-based site, corresponding information content and sensitivity ranges.

Station	HCl		HF	
	Microwindows and fitted interferences	DOFS ^a and sensitivity range	Microwindows, and fitted interferences	DOFS ^a and sensitivity range
Ny Ålesund	2727.60–2727.95 2925.80–2926.00 H ₂ O, O ₃ , CH ₄	3.85 10–41.3 km	4038.80–4039.15 H ₂ O, HDO, CH ₄	2.00 13.6–31.6 km
Thule	2727.60–2727.95 2775.60–2775.95 2925.7–2926.1 HDO, O ₃ , CH ₄	1.7 12.2–31.4 km	4000.80–4001.20 4038.75–4039.20 H ₂ O, HDO, CH ₄	1.7 12.2–31.4 km
Kiruna	2727.73–2727.82 2752.01–2752.05 2775.70–2775.79 2821.51–2821.62 2843.55–2843.65 2925.80–2926.00 2963.23–2963.35 3045.00–3045.10 H ₂ O, HDO, O ₃ , CH ₄	3.25 11.7–41.6 km	4000.9–4001.05 4038.85–4039.08 H ₂ O, HDO	3.07 11.7–41.6 km
Poker Flat	2925.80–2926.00 H ₂ O, O ₃ , CH ₄ , NO ₂	2.0 12–40 km	4038.80–4039.15 H ₂ O, HDO	1.9 14–40 km
Bremen	2727.60–2727.95 2925.80–2926.00 H ₂ O, O ₃ , CH ₄	2.78 10.0–39.2 km	4038.80–4039.15 H ₂ O, HDO, CH ₄	1.97 12.4–34.1 km
Jungfraujoch	2727.73–2727.83 2775.70–2775.80 2925.80–2926.00 O ₃ , CH ₄ , NO ₂	2.00±0.35 10–27 km	4038.8–4039.11 H ₂ O, HDO, CH ₄	1.80±0.20 12–27 km
Toronto	2925.80–2926.00 O ₃ , CH ₄ , NO ₂	3.10 14–39 km	4038.77–4039.13 H ₂ O, HDO, CH ₄	2.0 20–35 km
Izaña	Same as per Kiruna	2.35 11.7–41.6 km	Same as per Kiruna	1.95 11.7–41.6 km
Reunion Island	2843.3–2843.8 2925.7–2926.6 H ₂ O, O ₃ , CH ₄ , NO ₂	1.54±0.12 10.0–43.6 km	4038.7–4039.05 H ₂ O, HDO, CH ₄	1.51±0.06 14.8–39.2 km
Wollongong	2925.75–2926.05 H ₂ O, O ₃ , CH ₄ , NO ₂	1.72±0.11 14–36 km	4038.80–4039.05 H ₂ O, HDO, CH ₄	1.47±0.08 14–34 km
Lauder	2925.75–2926.05 H ₂ O, O ₃ , CH ₄	2.52±0.24 18–38 km	4038.78–4039.10 H ₂ O, HDO, CH ₄	2.67±0.21 14–36 km
Arrival Heights	2925.75–2926.05 H ₂ O, O ₃ , CH ₄	2.45±0.35 14–40 km		–

^a DOFS were computed using either typical averaging kernel or the actual subsets of matrices used for the smoothing process; in the latter case, the standard deviation around the mean is given.

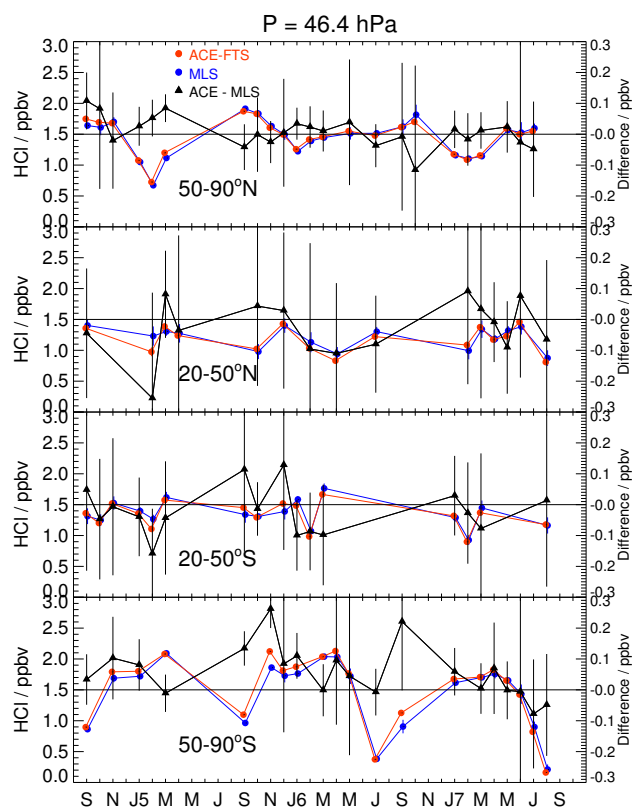


Fig. 1. Time series of HCl monthly mean mixing ratios at 46 hPa from ACE-FTS and Aura MLS in four latitude bins identified in each panel. The zonal means for each month and latitude bin are obtained by averaging all available coincident profiles from both data sets; gaps are largely caused by gaps in the reprocessing of MLS version 2.2 data, along with a few gaps in the ACE-FTS data. Black triangles are the differences (ACE-FTS minus MLS, see right axis scale). Mixing ratio error bars represent the 2- σ standard errors for the zonal means, based on the available single-profile error estimates; error bars for the differences are the root sum square of these estimated standard errors in the means.

are fewer ACE-FTS measurements available at tropical latitudes.

Determination of the altitude range for partial column comparisons were objectively based on averaging kernel and/or eigenvector inspections, following the practical methods described previously in Barret et al. (2003) and Vigouroux et al. (2007). The adopted values are listed in columns 3 and 5 of Table 3, for each site and for both reservoir species.

Densities have been computed using the pressure-temperature (p-T) information associated with each data set. For ACE-FTS, p-T profiles retrieved from the spectra (Sect. 2) and made available together with the vmr distributions were used. For ground-based FTIRs, the daily p-T information used in the PROFFIT or SFIT2 retrievals was adopted; they are either based on NCEP (National Centers

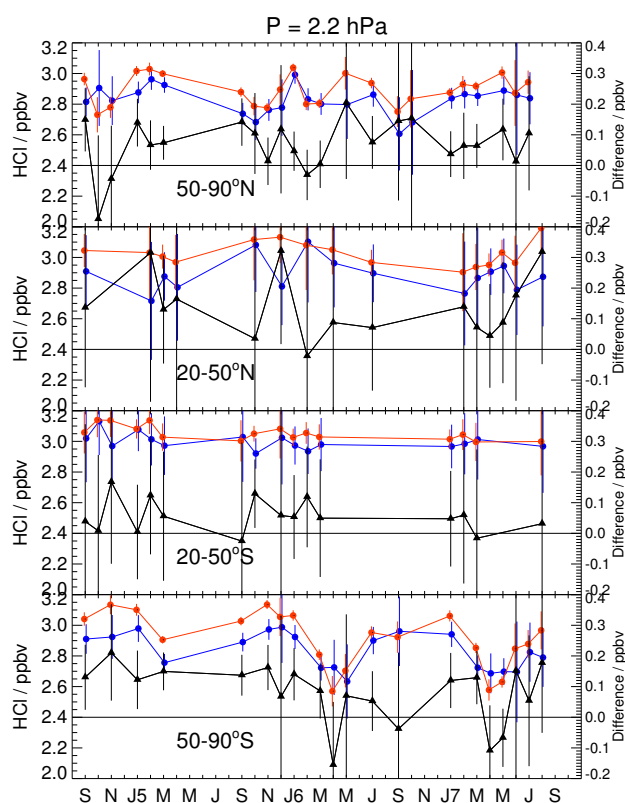


Fig. 2. Same as Fig. 1 but for 2.2 hPa.

for Environmental Prediction) data, or on p-T soundings performed in the vicinity of the site.

4 Comparisons between ACE-FTS measurements and correlative data

The following subsections will present the HCl, HF, CFC-11 and CFC-12 comparisons, starting with space-based instruments, then balloon-borne and ground-based FTIRs, in this order and when available.

Fractional differences (Δ) between the vmrs or partial columns from ACE-FTS and the validating instrument (VAL) have been computed using the following formula:

$$\Delta = 2 \times \frac{(x_{\text{ACE}} - x_{\text{VAL}})}{(x_{\text{ACE}} + x_{\text{VAL}})} \quad (\text{in } \%) \quad (2)$$

Relative differences are statistically characterized by the standard deviation around the mean (denoted σ) and the standard error on the mean (as σ/\sqrt{N} for N coincidences).

4.1 HCl comparisons

4.1.1 MLS

The version 2.2 ACE-FTS HCl profiles have been shown to agree quite well with MLS v2.2 HCl retrievals, within about

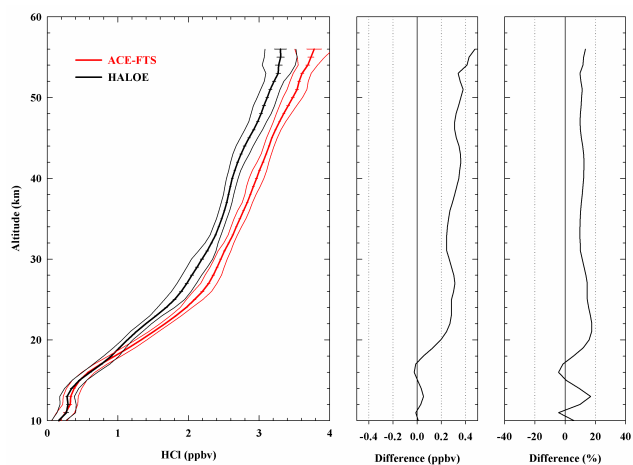


Fig. 3. Left panel: average profiles (thick lines) for all coincident measurements between ACE-FTS (red) and HALOE (black), as a function of altitude. Thin lines are the profiles of standard deviations ($1\text{-}\sigma$) of the distributions, while error bars (often too small to be seen) represent the standard error. Absolute differences based on all 36 coincidences are shown in the centre panel while fractional differences are reproduced on the right panel.

5 to 10% on average, from 100 to 0.2 hPa (i.e. approximately from 16 to 60 km) (Froidevaux et al., 2008); furthermore, the latitudinal distribution observed by MLS is well matched by that obtained from coincident ACE-FTS profiles. The above reference made use of data comparisons from mid-2004 through 2006; the results are essentially the same if one uses comparisons from 2007 alone, and they are not shown here. Instead, we show the time dependence of monthly zonal mean comparisons from all (4731) available coincident ACE-FTS and MLS profile pairs in Fig. 1, at the 46 hPa pressure level (around 20 km). The monthly mean HCl averages from ACE-FTS and MLS are in good agreement, as shown by the error bars ($2\text{-}\sigma$) on the abundances as well as the differences in Fig. 1. As one would expect, the number of monthly coincidences is largest for the high latitude bins (the maximum number being 285); the error bars in this figure give a good indication of the relative number of coincidences. Figure 2 provides a similar view for the upper stratosphere (at 2.2 hPa or about 41 km), where the variations are smaller, but nevertheless well matched between these two data sets. It should be pointed out that such time series comparisons are not meant to represent the best description of actual atmospheric variations versus time, as only coincident profile pairs, based on the ACE-FTS sampling pattern, are included; we simply demonstrate that similar temporal changes can be obtained from such matched profiles.

4.1.2 HALOE

Figure 3 shows the average HCl profiles measured by both instruments for all 36 available coincidences (left panel), i.e.

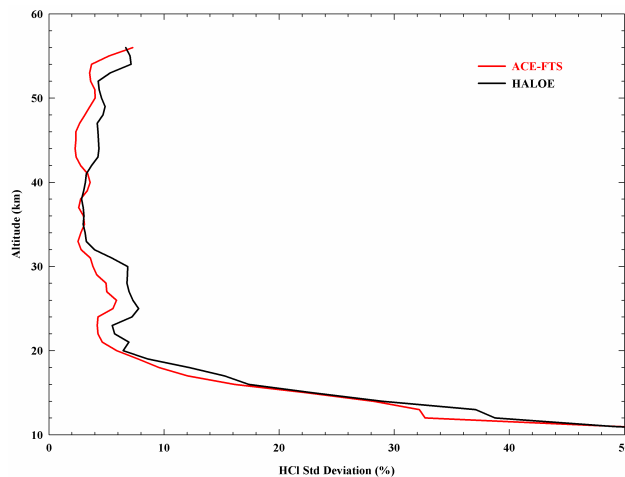


Fig. 4. Standard deviations of the distributions relative to the mean HCl vmr at each altitude, for all coincident events, for ACE-FTS (red) and HALOE (black).

considering simultaneously the sunset and sunrise events. Both instruments show vmrs increasing with altitude, with the ACE-FTS vmrs biased high compared to HALOE above about 20 km. The thin lines in left panel of Fig. 3 represent the standard deviations of the distribution of profiles measured by each instrument, indicating that both instruments measure similar variability. Measurement variability is quantified more clearly in Fig. 4, which shows the standard deviations of the distributions relative to the mean mixing ratios. There is excellent agreement between the standard deviations of ACE-FTS and HALOE at all altitudes, with values on the order of about 5% from 20 to 55 km.

The right panel of Fig. 3 shows the fractional differences as a function of altitude. Average differences are around 10–15% throughout the stratosphere, with the ACE-FTS biased high compared to HALOE above 17 km. This offset is commensurate with earlier intercomparisons (see Sect. 3.2), concluding that the HCl observations by HALOE are biased low with respect to other relevant data sets. This is also consistent with the conclusions from the MLS versus HALOE comparisons performed by Froidevaux et al. (2008). These authors have noted that, despite a systematic bias, the MLS and HALOE spatial variations are very similar and of the same amplitude and sign as the one derived here.

4.1.3 SPIRALE

After locating the ACE-FTS occultation that was closest to the SPIRALE measurement, an additional “coincidence criterion” was investigated. Using the MI-MOSA (Modélisation Isentrope du transport Mésoéchelle de l’Ozone Stratosphérique par Advection) contour advection model (Hauchecorne et al., 2002), potential vorticity (PV) maps in the region of both measurements have been

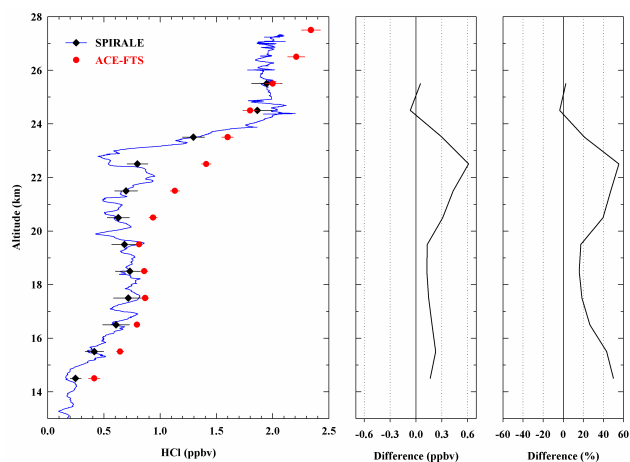


Fig. 5. HCl vertical profiles (on the left) obtained by ACE-FTS (from occultation sr13151, in red) and SPIRALE (in black and blue) on 20–21 January 2006, near Kiruna. The solid blue line corresponds to the SPIRALE measurements (very high vertical resolution) and the black diamonds correspond to the SPIRALE profile smoothed with a triangular function (see text). The centre panel shows absolute difference between the two profiles while corresponding relative differences (Δ) are presented on the right.

calculated at each hour between 17:00 UT on 20 January 2006 and 08:00 UT on 21 January 2006 on isentropic surfaces, every 50 K from 350 K to 800 K (corresponding to altitudes between 12.8 and 30 km). From these PV fields it can be deduced that SPIRALE and ACE-FTS vertical profiles were located in similar air masses in the well-established polar vortex over the whole range of altitudes. The dynamical situation was very stable with PV agreement better than 10%. Thus the meteorological situation was considered suitable to allow direct comparison between these two data sets.

Before performing any comparison, the difference in the vertical resolution of the two instruments had to be taken into account, because ACE-FTS has a vertical resolution of 3–4 km while that of SPIRALE is on the order of meters. A triangular weighting function of width equal to 3 km at the base (corresponding to the ACE-FTS estimated vertical resolution) was therefore applied to SPIRALE data at each of the ACE-FTS measurement altitudes, as in, e.g., Dupuy et al. (2008; Sect. 4, Eq. 1). Consequently, the SPIRALE profile was truncated by 1.5 km at the bottom and at the top. Then, the resulting profile was interpolated on to the ACE 1 km-grid. The ACE-FTS and SPIRALE HCl profiles (Fig. 5) are in good agreement between 16 and 20 km and above 23 km. Over these altitude ranges, the fractional differences (see right panel) lie between -2 and $+27\%$. The lower (by more than 40%) HCl values observed by SPIRALE in the layer 20–23 km height are probably due to a PSC crossed by the gondola from 19.3 to 20.7 km height (detected by the onboard aerosol counter). Indeed, the use of the HYSPLIT model (HYbrid Single-Particle Lagrangian Integrated

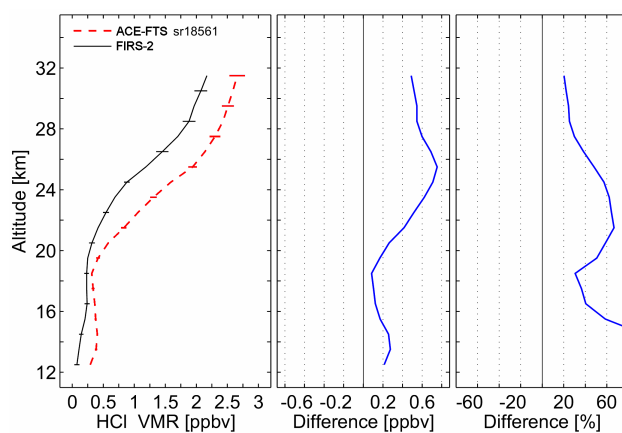


Fig. 6. Comparison of an HCl profile from FIRS-2 on 24 January 2007 at 10:11 UT with a profile from ACE-FTS occultation sr18561 obtained on 23 January 2007 at 08:25 UT. Left: Measured vmr profiles from FIRS-2 (solid black) and ACE-FTS (dashed red). Error bars show uncertainty estimate for FIRS-2 and fitting error for ACE-FTS every 2 km. Middle: Absolute differences in ppbv. Right: Fractional differences $2 \times (\text{ACE} - \text{FIRS-2}) / (\text{ACE} + \text{FIRS-2})$ in percent.

Trajectory, see <http://www.arl.noaa.gov/ready/hysplit4.html>) shows that the temperature encountered along the trajectories above 20.7 km during two days before the measurements were compatible with the formation of PSC particles, on which HCl may be adsorbed. At the time of the SPIRALE and of the aerosol counter measurements, the PSC has sedimented. In general, the ACE-FTS HCl vmr values are larger than those of SPIRALE for the whole altitude range except at 24.5 km.

4.1.4 FIRS-2

The comparison between ACE-FTS and FIRS-2 HCl profiles is shown in Fig. 6. ACE-FTS reports systematically more HCl over the altitude range 12–31 km, with largest fractional differences ($>+90\%$) below 15 km where the HCl abundance is small (less than 0.4 ppbv). Above 15 km, the profile shapes are similar for ACE-FTS and FIRS-2, but the ACE-FTS vmr values are significantly larger than those of FIRS-2. The fractional differences are within $+20$ to $+66\%$ with smallest values at the uppermost levels. There are also indications of a high bias for MLS versus FIRS-2 HCl profiles in Froidevaux et al. (2008), although it's hard to compare since these coincidences were obtained at different latitudes and seasons.

At present, the large difference between ACE-FTS and FIRS-2 remains unexplained. All eleven HCl lines used in the FIRS-2 retrievals provide consistent results over the whole altitude range. These measurements were indeed obtained further north with respect to ACE-FTS, and they were performed in PSCs. However, a feature at 20 km in the ACE-imager extinction profiles supports the idea that the

ACE-FTS observations could also have been influenced by PSCs, at least partially. Onboard the same gondola than FIRS-2, the Submillimeterwave Limb Sounder (SLS) measured large amounts of ClO. Although HCl measurements performed by SLS were also higher than FIRS-2, it was not by the amount suggested by the comparison performed here and part of the difference could result from real HCl variability in winter high latitude stratosphere, in particular when comparing vortex-edge and inside-of-vortex air masses.

4.1.5 Mark-IV

The comparison between ACE-FTS and MkIV HCl profiles is shown in Fig. 7. The ACE-FTS zonal mean vmrs are in very good agreement (to better than $\pm 7\%$) with the MkIV measurements above 20 km. Between 17 and 20 km, ACE-FTS reports less HCl than MkIV, by up to -20% . Below 17 km, the relative differences become extremely large. This is mostly due to very small vmr values for both ACE-FTS and MkIV.

4.1.6 Ground-based FTIRs

Individual site comparisons have been performed, on the basis of the coincidence criteria defined in Sect. 3.6. Statistical results consisting of the mean fractional differences, corresponding standard deviations and standard errors are listed in Table 4, except when only a few coincidences are available. The next column in Table 4 provides the number of coincidences; 174 ACE-FTS occultations are used here, recorded from March 2004 to March 2007. Furthermore, a global mean and corresponding statistics are given at the end of the table, for all coincidences considered at once. Although no clear picture emerges from the statistics, it should be pointed out that (i) very few relative differences are significant at the $1-\sigma$ level; (ii) no PV filtering is included while the largest positive differences (Δ ; see Eq. 2) are generally obtained for high latitude sites (Ny Ålesund and Arrival Heights); (iii) although two of the three negative mean values are observed in the Southern Hemisphere (Wollongong and Lauder), no conclusion should be drawn regarding a latitudinal pattern in the differences, given the uncertainties affecting the means.

The overall relative difference is $(6.9 \pm 15.9)\%$ ($1-\sigma$), or $(6.9 \pm 1.2)\%$ (standard error). This would suggest a slight overestimation of HCl partial columns by ACE-FTS, on the order of a few percent. We note however that the largest individual fractional differences, all observed at high northern and southern latitudes during the winter-spring time period, are included in this evaluation. In order to minimize the contribution of spatial variability on the global statistics, we have further limited the latitude difference to 200 km, with no additional restriction on the longitude spread. Corresponding statistics are given in the last line of Table 4. We note a significant improvement, with a mean Δ found equal to $(2.0 \pm 11.7)\%$ ($1-\sigma$), or $(2.0 \pm 1.8)\%$ (standard error).

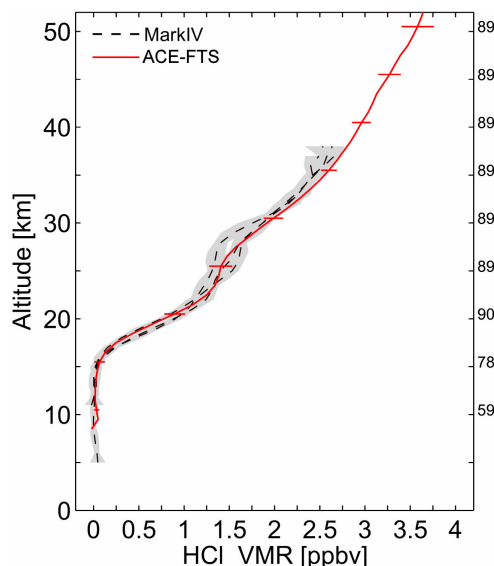


Fig. 7. Comparison of three HCl profiles from MkIV (20 September 2003 – 01:25 UT, 24 September 2004 – 01:00 UT and 21 September 2005 – 01:25 UT) around Fort Sumner (34.4° N, 104.2° W – New Mexico, USA), with a zonal average of all ACE-FTS profiles obtained in August, September and October 2004, 2005 and 2006 within a latitude bin of $\pm 5^\circ$ centered at 34.4° N. The ACE-FTS zonal mean profile is shown in red, with error bars corresponding to the $1-\sigma$ standard deviation of the mean. The individual measurements from MkIV are shown by the dashed black curves, with corresponding uncertainties given by the shaded area. The number of ACE-FTS occultations used in the zonal averages is indicated every 5 km on the right-hand side.

In addition, all coincident HCl partial columns from ACE-FTS and from all 12 ground-based sites involved here have been included in a scatter plot (Fig. 8). Sites are identified by various symbols and colors, data from all latitudes and seasons are included. It is worth mentioning that the magnitude of the partial columns is influenced by the altitude ranges considered at each site in the partial column calculations (see Table 3 and Sect. 3.6). Moreover, measurements are not performed year-round at all sites. Hence, no direct conclusion should be drawn from their relative values and distribution.

The linear regression to all data is reproduced by the dash-dotted black line, its slope and intercept are respectively equal to 0.90 and 5.52×10^{14} molecules/cm², with a correlation coefficient R of 0.87. When restricting the data set to coincidences occurring within less than 200 km of latitude difference (see continuous black line and crossed-symbols), the correlation improves significantly with a slope of 1.02, an intercept of 2.25×10^{13} molecules/cm² and a correlation coefficient of 0.96. This fitted straight line is compatible with the 1:1 line correlation, at the 95% confidence level. This improvement suggests that part of the comparisons still include natural spatial variability for HCl, in particular in vortex-type situations, where subsided or chlorine-depleted air might be

Table 4. Fractional differences between ACE-FTS and ground-based partial column measurements of HCl and HF, together with standard deviations and standard errors on the means. The number of coincidences is given in columns 3 and 5. The last two lines provide the statistical parameters considering all coincidences at once, within 1000 km (500 km for Kiruna and Thule, 1200 km for Reunion Island) and when further restricting latitude difference to less than 200 km, respectively.

Station	HCl		HF	
	Mean Δ (%) 1- σ and [stand. error]	# coinc.	Mean Δ (%) 1- σ and [stand. error]	# coinc.
Ny Ålesund	15.45±19.29 [4.21]	21	12.34±7.74 [2.00]	15
Thule	2.19±9.46 [2.85]	11	6.54±7.42 [1.98]	14
Kiruna	9.77±8.35 [2.23]	14	6.60±9.58 [2.76]	12
Poker Flat	7.1±10.02 [2.90]	12	6.96±7.94 [2.12]	14
Bremen	12.16±15.09 [4.03]	14	–	–
Jungfraujoch	10.76±12.75 [2.50]	26	7.42±10.88 [2.43]	20
Toronto	6.20±12.95 [3.46]	14	–	5
Izaña	–	5	–	4
Reunion Island	–	5	–	2
Wollongong	−5.68±16.88 [3.46]	8	–	4
Lauder	−2.84±6.25 [1.33]	22	13.54±9.34 [2.20]	18
Arrival Heights	8.41±25.38 [5.41]	22	–	–
All	6.95±15.94 [1.21]	174	7.40±11.38 [1.10]	108
Lat.diff. <200 km	2.03±11.74 [1.81]	42	2.80±8.70 [1.59]	30

sampled. This is consistent with the statistically significant drop between the actual ranges of the fractional differences, from (5.8 to 7.8) % to (0.2 to 3.8) % reported here above (see Table 4, $\Delta \pm$ standard error). If we assume that the closest comparisons are not significantly affected by spatial variability, we can evaluate that at least a third of the fractional differences characterizing the complete dataset can be attributed to natural variability. The remaining contribution corresponds to a negligible up to a reasonable bias between the ground-based FTIRs and the ACE-FTS partial columns, of less than 4%. Hence, the latter value has to be considered as the most representative upper limit bias between the space- and the ground-based instruments. Also, it should be noted that restriction of the time differences (e.g., to ± 12 h) does not improve the correlation.

4.2 HF comparisons

4.2.1 HALOE

Similarly to Fig. 3, Fig. 9 shows the average HF profiles measured by both instruments for all coincidences, in left panel. Here again, results for averages over all of the coincidences are reported. Both instruments show very similar profile shapes, but the ACE-FTS vmrs are biased high compared to HALOE throughout most of the altitude range. Qualitatively, it is clear that both instruments measure similar variability below 30 km, but that ACE-FTS variability is higher above 30 km. Measurement variability is quantified more clearly in Fig. 10. As noted above, the ACE-FTS instrument shows

higher variability above 30 km, probably indicative of poorer precision. Nevertheless, the standard deviation profiles have similar shapes, with both instruments measuring an increase in variability near 30 km. This suggests that the larger variability near 30 km is a real geophysical feature. Although not shown here, this is analogous to the standard deviations seen in e.g., the CH₄ comparisons (De Mazière et al., 2008). We believe that this is likely the result of summertime longitudinal variations arising from differential meridional transport caused by breaking of westward-propagating waves that are evanescent in the summer easterly flow (e.g., Hoppel et al., 1999).

The right panel of Fig. 9 shows the percent differences between the instruments while the centre panel shows the absolute differences. Measurements from the ACE-FTS are biased high compared to HALOE, with mean differences around 5–20% from 15 to 49 km. As for HCl, the HF concentration measurements by HALOE have consistently revealed low biases when compared to other independent relevant datasets (i.e., Russell et al., 1996b; McHugh et al., 2005), whose magnitude is confirmed here.

4.2.2 FIRS-2

The results of the comparison for HF are shown in Fig. 11. ACE-FTS is systematically biased high with respect to FIRS-2. The extremely large relative differences at the lowest altitude levels (>100% below 17 km) can be explained by the very low values of the HF vmr at these altitudes, and by the negative vmr values (below 16 km) found

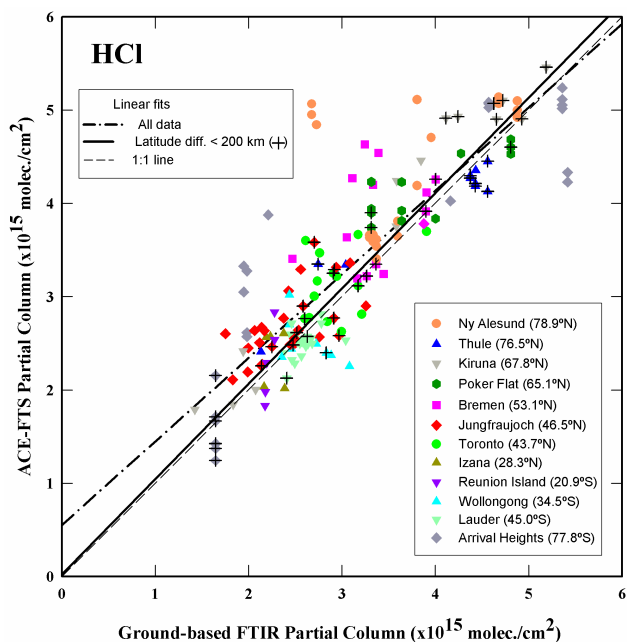


Fig. 8. Scatter plot of the ACE-FTS partial columns versus the ground-based coincident measurements, taken within ± 24 h and 1000 km (restricted to 500 km for Kiruna and Thule, relaxed to 1200 km for Reunion Island, see text). See inserted legend for identification of the sites. Linear fit to all data points is reproduced as a dash-dotted black line. When restricting latitudinal difference to less than 200 km (see symbols with pluses), the correlation is improved, with a linear fit (continuous black line) close to the 1:1 line (dashed line).

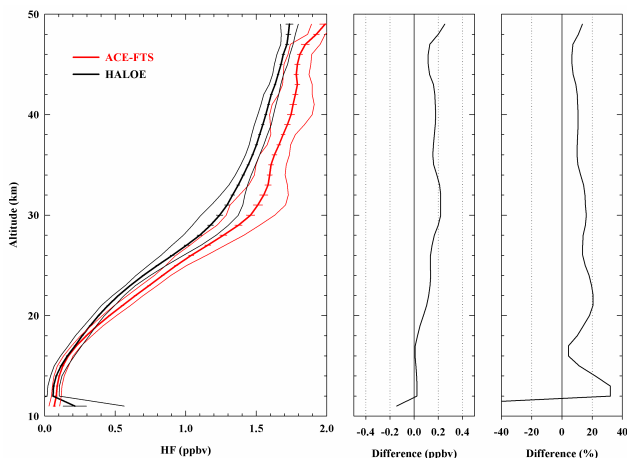


Fig. 9. Same as Fig. 3 but for comparison of HF profiles from HALOE and ACE-FTS.

in the FIRS-2 profile. This is also the range where the FIRS-2 quoted uncertainties are the largest ($\sim 60\%$). Above 17–18 km, significant differences ranging between +17 and +50% are found, i.e., in any case larger than the 10% uncertainty estimates for FIRS-2. Although smaller than for the

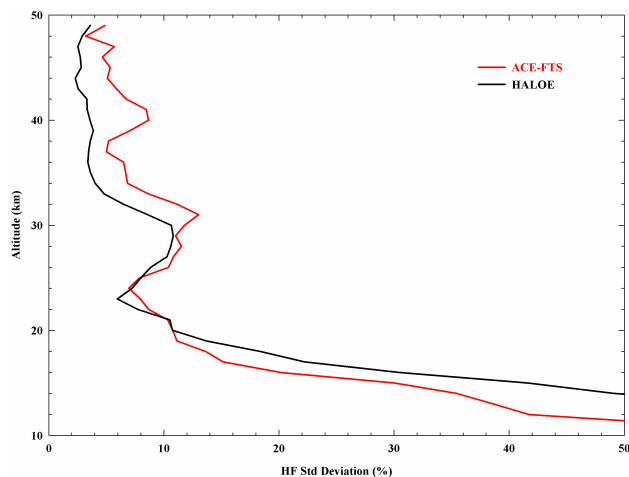


Fig. 10. Same as Fig. 4 but for comparison of HF profiles from HALOE and ACE-FTS.

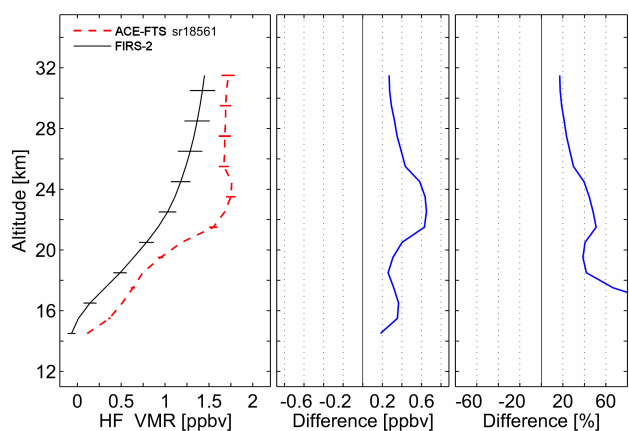


Fig. 11. Same as Fig. 6 but for comparison of HF profiles from FIRS-2 and ACE-FTS.

HCl comparison, the HF differences remain significant over the whole altitude range. This is unexplained thus far, and such similar discrepancies are not confirmed when looking at ozone (Dupuy et al., 2008; Fig. 26).

4.2.3 Mark-IV

The results of the comparison for HF are shown in Fig. 12. Here also, there is good agreement between the ACE-FTS vmrs and MkIV. The relative differences are within $\pm 10\%$ above 19 km. For the same reasons as mentioned for HCl in Sect. 4.1.5, the discrepancies increase rapidly below this altitude.

4.2.4 Ground-based FTIRs

The same approach has been used to compare ACE-FTS and ground-based FTIR partial columns of HF. The last two

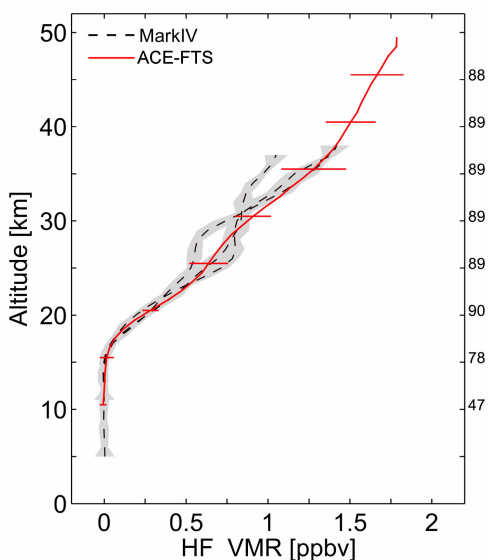


Fig. 12. Same as for Fig. 7 but for comparison of HF profiles from MkIV and ACE-FTS.

columns of Table 4 give the corresponding statistical results and number of available coincidences, found between March 2004 and December 2006, using the same temporal and spatial criteria as before. Here again, most results are compatible with a no bias at the $1\text{-}\sigma$ level, although the number of coincidences is generally lower than for HCl. When considering all data together, we found a mean relative difference and corresponding standard deviation of $(7.4\pm 11.4)\%$ ($1\text{-}\sigma$); or $(7.4\pm 1.1)\%$ (standard error). As for the HCl comparison, restriction of the dataset by considering maximum latitude difference of 200 km significantly reduces the mean bias to $(2.8\pm 8.7)\%$ ($1\text{-}\sigma$) and $(2.8\pm 1.6)\%$ (standard error), respectively.

Similarly to Fig. 8, Fig. 13 shows the HF partial column scatter plot. No direct comparison should be made between the HCl and HF scatter plots and data point distributions, as ground-based observations of these two species are not performed simultaneously, and HF is currently not available from all sites involved in our study. We notice that the distribution of the 108 data points is already quite compact. The linear regression yields a slope of 1.05, an intercept of 0.43×10^{14} molecules/cm² and a correlation coefficient of 0.96. Corresponding parameters indicate that the correlation is not improved when restricting the dataset to the 30 closer measurements in latitude (symbols with plusses), with values of 0.94, 1.37×10^{14} molecules/cm² and 0.96, respectively. Here again, this fitted function is compatible with the 1:1 line correlation, at the 95% confidence level. Contrary to the HCl comparisons, chemical activation cannot be invoked to explain dissimilarities between in- and out-of-vortex air masses, but the impact of vertical dynamical motion could result in large partial column differences. Such situations

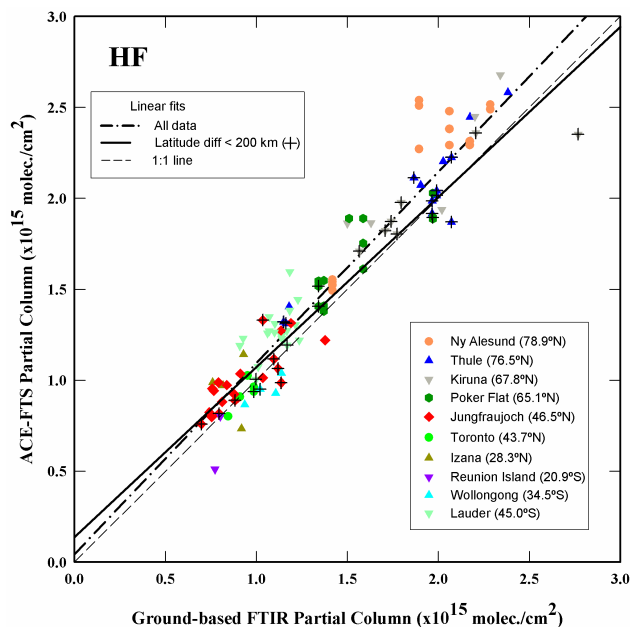


Fig. 13. Same as Fig. 8, but for comparison of ACE-FTS and ground-based FTIR partial columns for HF.

might have been encountered for a series of points corresponding to winter-spring time measurements above high-latitude sites of the Northern Hemisphere. As per HCl (see Sect. 4.1.6), the improvement noted for the mean fractional difference, from (6.3 to 8.5) % to (1.2 to 4.4) %, is consistent with a significant contribution of natural spatial variability to the bias computed with the relaxed collocation criteria. For HF, the upper limit bias between the ACE-FTS and the ground-based FTIR instruments is lower than 5%. Overall conclusions are unchanged if measurements closer in time are considered.

4.3 CFC-11 comparisons

4.3.1 FIRS-2

The CFC-11 comparison results are presented in Fig. 14. There is a very good agreement below 16 km with differences smaller than -10% (-20 pptv) from 12 to 16 km, with ACE-FTS reporting slightly smaller CFC-11 vmrs than FIRS-2. Above 16 km, the fractional differences increase with increasing altitude, up to $\sim -87\%$ at 19 km. It should be noted that these differences consistently remain within the uncertainty estimates for the FIRS-2 profile.

4.3.2 Mark-IV

Figure 15 shows the results of the CFC-11 comparison. The agreement is quite good. However, ACE-FTS vmr values are systematically smaller than those of MkIV, with differences

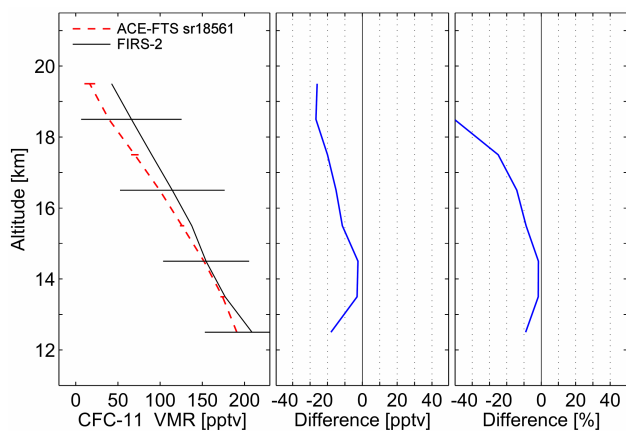


Fig. 14. Same as Fig. 6 but for comparison of CFC-11 (CCl₃F) profiles from FIRS-2 and ACE-FTS.

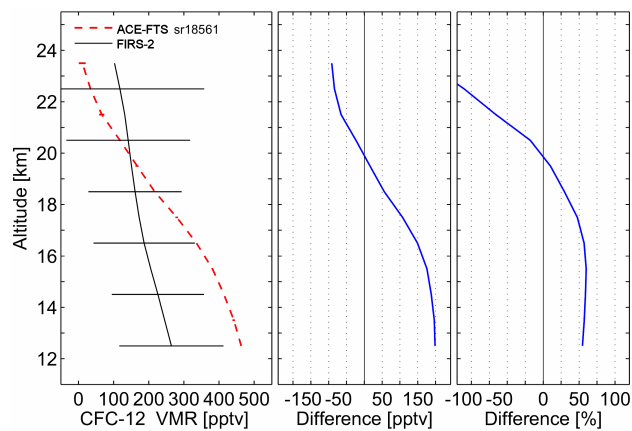


Fig. 16. Same as Fig. 6 but for comparison of CFC-12 (CCl₂F₂) profiles from FIRS-2 and ACE-FTS.

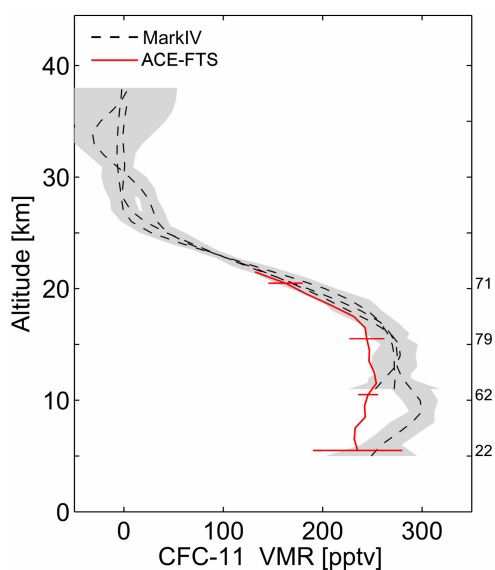


Fig. 15. Same as Fig. 7 but for comparison of CFC-11 (CCl₃F) profiles from MkIV and ACE-FTS.

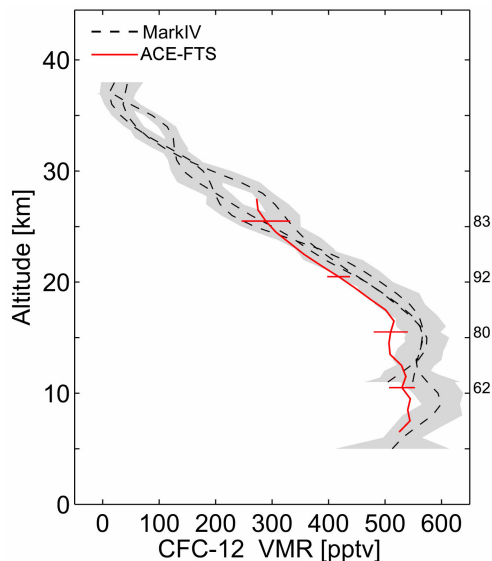


Fig. 17. Same as Fig. 7 but for comparison of CFC-12 (CCl₂F₂) profiles from MkIV and ACE-FTS.

on the order of -10% above 12 km and increasing to larger values (about -20%) below.

4.4 CFC-12 comparisons

4.4.1 FIRS-2

The ACE-FTS – FIRS-2 comparison for CFC-12 is shown in Fig. 16. Here, the vmr profiles for ACE-FTS and FIRS-2 have different shapes. The FIRS-2 profile has large uncertainty and shows only a slight decrease with increasing altitude, while the ACE-FTS vmr profile is more similar to that of CFC-11. Relative differences are positive (ACE-FTS vmrs larger than FIRS-2) from 12 to 20 km, with values close to $+50\%$ up to 17 km and decreasing quickly above. In the al-

titude range 17–24 km, the differences decrease with increasing altitude from $+48\%$ ($+108$ pptv) to -160% (-91 pptv) at the top of the comparison altitude range.

4.4.2 Mark-IV

Lastly, the ACE-FTS – MkIV comparison for CFC-12 is shown in Fig. 17. The differences are similar to the results found for CFC-11, with ACE-FTS vmrs systematically lower than MkIV but with maximum differences on the order of -10% . These negative differences in the CFCs comparisons with MkIV are consistent with the low biases noted in the comparison with FIRS-2.

5 Conclusions

In this paper, we have compared ACE-FTS v2.2 products with a series of available coincident or comparable profile or column measurements performed from space, balloons and from the ground, for HCl, HF, CFC-11 and CFC-12. Broad latitudinal and time coverage has been achieved for the reservoir species, with co-located measurements obtained from March 2004 to August 2007, from high-northern to high-southern latitudes, including sub-tropical and mid-latitude regions of both hemispheres.

For HCl, we have confirmed the very good agreement found by Froidevaux et al. (2008) between the ACE-FTS and MLS v2.2 data, when including the latest available 2007 coincidences. Related comparison of vmr profiles between 100 and 0.2 hPa (16 to 60 km) indicates very good consistency, with bias lower than 5%, and with no significant altitude pattern over this broad range of altitudes. Time series of monthly mean vmrs show very good agreement, in latitude, altitude and time. Statistical comparison with 36 HALOE v19 coincident HCl measurements suggests a systematic bias between both instruments, with the ACE-FTS vmrs 10 to 15% larger than those of HALOE over the whole stratosphere. The variability captured by both space instruments is, however, in very good agreement.

ACE-FTS HCl vmr profiles have been further compared with balloon-borne measurements. A single coincidence with a SPIRALE high-vertical resolution measurement performed near 67° N in January 2006 is also included. A good agreement (better than ~20%) is found between retrieved in situ HCl vmrs from 16 to 20 km and above 23 km. Below 16 km and between 20 and 23 km, we found the largest differences (ACE-FTS being higher), of more than 40%, and thus larger than combined uncertainties of both experiments. The analysis of the PV field does not suggest that large atmospheric inhomogeneities in sounded vortex air account for the observed discrepancies, but the presence of a PSC detected in situ by SPIRALE may explain the disagreement in the height range 20–23 km. Comparison with a single FIRS-2 profile obtained near 68° N in January 2007 shows large differences, from 0.1 to 0.7 ppbv (i.e., with ACE-FTS always larger by at least 20%, and up to 65%, relative to FIRS-2) in the 13 to 31 km altitude range. An ACE-FTS zonal mean profile was compared with three MkIV observations obtained in the fall of 2004 and 2005 around 35° N. Very good agreement to better than ±7% is obtained above 20 km and hence lower than the MkIV estimated uncertainty of ±10%. The agreement is less satisfactory at lower altitudes, where the HCl vmrs decrease rapidly while the corresponding uncertainties for both instruments are rapidly increasing.

Finally, comparisons of stratospheric partial columns were performed with NDACC FTIR data, collected over a wide range of latitudes. To minimize the impact of spatial natural variability of HCl on the computed differences, we have considered together coincident measurements taken within less

than 24h and at maximum latitude difference of 200 km. We found a compact correlation between ACE-FTS and gb-FTIR data, with a correlation coefficient (R) of 0.96, a slope of 1.02 and an intercept of 2.25×10^{13} molecules/cm². The same group of points suggests that ACE-FTS might be slightly biased high, with a mean fractional difference of (2.0 ± 1.8) % (standard error), at worst by about 4%.

The same set of coincident measurements from ACE-FTS and HALOE was used for HF comparisons. On average, they indicate that ACE-FTS provides similarly shaped profiles, but larger by 5 to 20% in the 15–49 km range, which is in line with earlier HALOE-related intercomparisons discussed in Sect. 3.2. Both instruments show further evidence of larger HF variability around 30 km, which is believed to be a real geophysical characteristic of the data sets used here. Similarly to the HCl comparison, the FIRS-2 vertical distribution systematically shows lower vmr values for HF (0.2 to 0.6 ppbv), with relative differences exhibiting similar vertical structure but lower amplitudes, generally between 20 and 50%. In contrast, zonal mean comparisons with MkIV data yield good agreement above 19 km, the relative differences being smaller than ±10%, i.e., in line with the 10% error associated to these balloon-borne measurements.

ACE-FTS and gb-FTIR HF partial columns have also been compared. As per HCl, only the tighter spatial coincidences have been considered to determine the mean relative difference between both datasets and corresponding statistics, here equal to (2.8 ± 1.6) % (standard error). The scatter plot based on the same 30 coincidences shows a compact correlation, with R equal to 0.96, a slope and an intercept of 0.94 and 1.37×10^{14} molecules/cm², respectively.

For CFC-11 and CFC-12, there was less data available for comparison with ACE-FTS. Single comparisons with a FIRS-2 flight and zonal mean comparison with MkIV data suggest however that the ACE-FTS vmr vertical distributions are reasonably good, although they generally seem to be lower in most of the altitude range, i.e., between 12 and 20 km. However, the low number of coincidences for both CFC-11 and CFC-12 limits the significance of these findings.

Overall, and when excluding the single SPIRALE and FIRS-2 measurements, which may have sampled significantly different air masses than ACE-FTS, the various comparisons indicate a good agreement for HCl with MLS, the NDACC FTIRs and MkIV, with averaged differences always lower than 10%. Comparison with HALOE would suggest larger positive values (10–15%), however HALOE profiles are known to be biased low, so that the actual differences are likely to be much smaller. For HF, we have less data available. Comparisons with the gb-FTIRs and MkIV also indicate agreement within 10%. Here again, HALOE indicate larger HF differences (10–20%) whose magnitudes might not be representative. Most of the differences are clearly attributable to the bias affecting the HALOE data. Hence, this intercomparison exercise indicates a generally good agreement to better than 5–10% for HCl and HF, with available

reference data sets, i.e., within the uncertainties affecting both ensembles. It should be noted that these uncertainties are valid for HCl and HF measurements taken down to about 20 km. Below this altitude, it is anticipated that the precision of the measurements will rapidly drop with decreasing altitude and vmr values. The lowermost ACE-FTS measurements available for HCl and HF should therefore be considered with care by the data users. No significant latitude or altitude difference was found when considering the various comparisons, covering a broad range of latitudes and seasons. It is therefore possible to capture natural atmospheric variability as well as particular events, using these measurements. Moreover, the results appear to be consistent over the three years of ACE-FTS data available at the time of writing, with no apparent degradation over time, allowing assessment of longer-term changes. For CFCs, the limited number of data sets for comparison did not allow us to derive statistically reliable results. Nevertheless, we estimated that the differences stay within 20% in most of the altitude ranges accessible to ACE-FTS, in particular for CFC-11.

Acknowledgements. Work at University of Liège was primarily supported by the Belgian Federal Science Policy Office (PRODEX Programme), Brussels. We thank the International Foundation High Altitude Research Stations Jungfrauoch and Gornergrat (HFSJG, Bern) for supporting the facilities needed to perform the observations. We further acknowledge the vital contribution from all colleagues in performing the ground-based observations used here. We would also like to thank Olivier Flock and Diane Zander for programming and secretarial supports, respectively.

The Atmospheric Chemistry Experiment (ACE), also known as SCISAT, is a Canadian-led mission mainly supported by the Canadian Space Agency (CSA) and the Natural Sciences and Engineering Research Council (NSERC) of Canada.

The authors thank the HALOE Science and Data Processing Teams for providing the profiles used in this work.

All the ground-based FTIR stations operate within the framework of the Network for the Detection of Atmospheric Composition Change (NDACC, see <http://www.ndacc.org>), and are nationally funded and supported.

The National Center for Atmospheric Research is supported by the National Science Foundation. The NCAR FTIR observation program at Thule, GR is supported under contract by the National Aeronautics and Space Administration (NASA).

The University of Bremen acknowledges financial support by the ESA project TASTE.

The support by the local Swedish Institute of Space Physics (IRF) staff in Kiruna is highly appreciated.

Work at the Toronto Atmospheric Observatory was supported by NSERC, Canadian Foundation for Climate and Atmospheric Sciences, ABB Bomem, Ontario Research and Development Challenge Fund, the Premier's Research Excellence Award, the University of Toronto, and a grant from the CSA.

The NIWA contribution to this study work was conducted within the FRST funded Drivers and Mitigation of Global Change programme (C01X0204). Support and logistics for the ground based

measurements FTIR at Arrival Heights was supplied by Antarctica New Zealand. We would like to thank Greg Bodeker for allowing us access to his "Potential Vorticity" database.

The SPIRALE balloon measurements could only be performed thanks to the technical team (L. Pomathiod, B. Gaubicher, G. Jannet); the flight was funded by ESA and French space agency CNES for the ENVISAT validation project; the CNES balloon launching team is greatly acknowledged for successful operations. A. Hauchecorne is acknowledged for making available the use of MIMOSA advection model and F. Coquelet for useful help in the PV calculations and ACE data formatting.

Work at the Jet Propulsion Laboratory, California Institute of Technology, was done under contract with NASA. We thank the Columbia Scientific Balloon Facility (CSBF) for the balloon flights whose data are used in this work.

Cora Randall contribution was funded by NASA grant NNG04GF39G. We would like to thank Lynn Harvey (LASP) who processed all the ACE data into a suitable format for the ACE vs HALOE comparisons.

Financial support by the EU-projects SCOUT, GEOMON and HYMN is further acknowledged.

Edited by: A. Richter

References

- Ackerman, M., Frimout, D., Girard, A., Gottignies, M., and Muller, C.: Stratospheric HCl from infrared spectra, *Geophys. Res. Lett.*, 3, 81–83, 1976.
- Anderson, J., Russell, J. M., Solomon, S., and Deaver, L. E.: HALOE confirmation of stratospheric chlorine decreases in accordance with the Montreal protocol, *J. Geophys. Res.*, 105, 4483–4490, 2000.
- Barret, B., De Mazière, M., and Mahieu, E.: Ground-based FTIR measurements of CO from the Jungfrauoch: characterisation and comparison with in situ surface and MOPITT data, *Atmos. Chem. Phys.*, 3, 2217–2223, 2003, <http://www.atmos-chem-phys.net/3/2217/2003/>.
- Bernath, P. F., McElroy, C. T., Abrams, M. C., Boone, C. D., Buttler, Camy-Peyret, C., Carleer, M., Clerbaux, C., Coheur, P.-F., Colin, R., DeCola, P., De Mazière, M., Drummond, J. R., Dufour, D., Evans, W. F. J., Fast, H., Fussen, D., Gilbert, K., Jennings, D. E., Llewellyn, E. J., Lowe, R. P., Mahieu, E., McConnell, J. C., McHugh, M., McLeod, S. D., Michaud, R., Midwinter, C., Nassar, R., Nichitui, F., Nowlan, C., Rinsland, C. P., Rochon, Y. J., Rowlands, N., Semeniuk, K., Simon, P., Skelton, R., Sloan, J. J., Soucy, M.-A., Strong, K., Tremblay, P., Turnbull, D., Walker, K. A., Walkty, I., Wardle, D. A., Wehrle, V., Zander, R., and Zou, J.: Atmospheric Chemistry Experiment (ACE): mission overview, *Geophys. Res. Lett.*, 32, L15S01, doi:10.1029/2005GL022386, 2005.
- Boone, C. D., Nassar, R., Walker, K. A., Rochon, Y., McLeod, S. D., Rinsland, C. P., and Bernath, P. F.: Retrievals for the atmospheric chemistry experiment Fourier-transform spectrometer, *Appl. Opt.*, 44, 7218–7218, 2005.
- Châteauneuf, F. J., Fortin, S. Y., Bujis, H. L., Soucy, M.-A. A.: On-orbit performance of the ACE-FTS instrument, in: *Proceed-*

- ings of SPIE, Vol. 5542, Earth Observing systems IX, edited by: Barnes, W. L. and Butler, J. J. (Bellingham, WA), 2004.
- Connor, B. J., Jones, N. B., Wood, S. W., Keys, J. G., Rinsland, C. P., and Murcray, F. J.: Retrieval of HCl and HNO₃ profiles from ground-based FTIR data using SFIT2. Atmospheric ozone, Proceedings of the XVIII Quadrennial Ozone Symposium, L'Aquila, Italy, September 1996, Vol. 2, edited by: Bojkov, R. D. and Visconti, G., 485–487, 1998.
- Chipperfield, M. P., Burton, M., Bell, W., Paton Walsh, C., Blumenstock, T., Coffey, M. T., Hannigan, J. W., Mankin, W. G., Galle, B., Mellqvist, J., Mahieu, E., Zander, R., Notholt, J., Sen, B., and Toon, G. C.: On the use of HF as a reference for the comparison of stratospheric observations and models, *J. Geophys. Res.*, 102, 12901–12919, 1997.
- De Mazière, M., Vigouroux, C., Bernath, P. F., Baron, P., Blumenstock, T., Boone, C., Brogniez, C., Catoire, V., Coffey, M., Duchatelet, P., Griffith, D., Hannigan, J., Kasai, Y., Kramer, I., Jones, N., Mahieu, E., Manney, G. L., Piccolo, C., Randall, C., Robert, C., Senten, C., Strong, K., Taylor, J., Tétard, C., Walker, K. A., and Wood, S.: Validation of ACE-FTS v2.2 methane profiles from the upper troposphere to the lower mesosphere, *Atmos. Chem. Phys.*, 8, 2421–2435, 2008, <http://www.atmos-chem-phys.net/8/2421/2008/>.
- Dupuy, E., Walker, K. A., Kar, J., Boone, C. D., McElroy, C. T., Bernath, P. F., Drummond, J. R., Skelton, R., McLeod, S. D., Hughes, R. C., Nowlan, C. R., Dufour, D. G., Zou, J., Nichitiu, F., Strong, K., Baron, P., Bevilacqua, R. M., Blumenstock, T., Bodeker, G. E., Borsdorff, T., Bourassa, A. E., Bovensmann, H., Boyd, I. S., Bracher, A., Brogniez, C., Burrows, J. P., Catoire, V., Ceccherini, S., Chabrilat, S., Christensen, T., Coffey, M. T., Cortesi, U., Davies, J., De Clercq, C., Degenstein, D. A., De Mazière, M., Demoulin, P., Dodion, J., Firanski, B., Fischer, H., Forbes, G., Froidevaux, L., Fussen, D., Gerard, P., Godin-Beekman, S., Goutail, F., Granville, J., Griffith, D., Haley, C. S., Hannigan, J. W., Höpfner, M., Jin, J. J., Jones, A., Jones, N. B., Jucks, K., Kagawa, A., Kasai, Y., Kerzenmacher, T. E., Kleinböhl, A., Klekociuk, A. R., Kramer, I., Küllmann, H., Kutippurath, J., Kyrölä, E., Lambert, J.-C., Livesey, N. J., Llewellyn, E. J., Lloyd, N. D., Mahieu, E., Manney, G. L., Marshall, B. T., McConnell, J. C., McCormick, M. P., McDermid, I. S., McHugh, M., McLinden, C. A., Mellqvist, J., Mizutani, K., Murayama, Y., Murtagh, D. P., Oelhaf, H., Parrish, A., Petelina, S. V., Piccolo, C., Pommereau, J.-P., Randall, C. E., Robert, C., Roth, C., Schneider, M., Senten, C., Steck, T., Strandberg, A., Strawbridge, K. B., Sussmann, R., Swart, D. P. J., Tarasick, D. W., Taylor, J. R., Tétard, C., Thomason, L. W., Thompson, A. M., Tully, M. B., Urban, J., Vanhellemont, F., von Clarmann, T., von der Gathen, P., von Savigny, C., Waters, J. W., Witte, J. C., Wolff, M., and Zawodny, J. M.: Validation of ozone measurements from the Atmospheric Chemistry Experiment (ACE), *Atmos. Chem. Phys. Discuss.*, 8, 2513–2656, 2008, <http://www.atmos-chem-phys-discuss.net/8/2513/2008/>.
- Farmer, C. B., Raper, O. F., and Norton, R. H.: Spectroscopic detection and vertical distribution of HCl in the troposphere and stratosphere, *Geophys. Res. Lett.*, 3, 13–16, 1976.
- Froidevaux, L., Livesey, N. J., Read, W. G., Jiang, Y. B., Jimenez, C., Filipiak, M. J., Schwartz, M. J., Santee, M. L., Pumphrey, H. C., Jiang, J. H., Wu, D. L., Manney, G. L., Drouin, B. J., Waters, J. W., Fetzer, E. J., Bernath, P. F., Boone, C. D., Walker, K. A., Jucks, K. W., Toon, G. C., Margitan, J. J., Sen, B., Christensen, L. E., Elkins, J. W., Atlas, E., Lueb, R. A., and Hendershot, R.: Early validation analyses of atmospheric profiles from EOS MLS on the Aura satellite, *IEEE Trans. Geosci. Remote Sens.*, 44(5), 1106–1121, doi:10.1109/TGRS.2006.864366, 2006a.
- Froidevaux, L., Livesey, N. J., Read, W. G., Salawitch, R. J., Waters, J. W., Drouin, B., MacKenzie, I. A., Pumphrey, H. C., Bernath, P., Boone, C., Nassar, R., Montzka, S., Elkins, J., Cunnold, D., and Waugh, D.: Temporal decrease in upper atmospheric chlorine, *Geophys. Res. Lett.*, 33, L23813, doi:10.1029/2006GL027600, 2006b.
- Froidevaux, L., Jiang, Y. B., Lambert, A., Livesey, N. J., Read, W. G., Waters, J. W., Fuller, R. A., Marcy, T. P., Popp, P. J., Gao, R. S., Fahey, D. W., Jucks, K. W., Stachnik, R. A., Toon, G. C., Christensen, L. E., Webster, C. R., Bernath, P. F., Boone, C. D., Walker, K. A., Pumphrey, H. C., Harwood, R. S., Manney, G. L., Schwartz, M. J., Daffer, W. H., Drouin, B. J., Cofield, R. E., Cuddy, D. T., Jarnot, R. F., Knosp, B. W., Perun, V. S., Snyder, W. V., Stek, P. C., Thurstans, R. P., and Wagner, P. A.: Validation of Aura Microwave Limb Sounder HCl measurements, *J. Geophys. Res.*, 113, D15S25, doi:10.1029/2007JD009025, 2008.
- Gilbert, K. L., Turnbull, D. N., Walker, K. A., Boone, C. D., McLeod, S. D., Butler, M., Skelton, R., Bernath, P. F., Châteauneuf, F., and Soucy, M.-A.: The onboard imagers for the Canadian ACE SCISAT-1 mission, *J. Geophys. Res.*, 112, D12207, doi:10.1029/2006JD007714, 2007.
- Goldman, A., Paton-Walsh, C., Bell, W., Toon, G. C., Blavier, J. F., Sen, B., Coffey, M. T., Hannigan, J. W., and Mankin, W. G.: Network for the Detection of Stratospheric Change Fourier transform infrared intercomparison at Table Mountain Facility, *J. Geophys. Res.*, 104, 30481–30504, 1999.
- Griffith, D. W. T., Jones, N. B., McNamara, B., Paton-Walsh, C., Bell, W., and Bernardo, C.: Intercomparison of ground-based solar FTIR measurements of atmospheric gases at Lauder, New Zealand, *J. Atmos. Oceanic Technol.*, 20, 1138–1153, 2003.
- Gunson, M. R., Abrams, M. C., Lowes, L. L., Mahieu, E., Zander, R., Rinsland, C. P., Ko, M. K. W., Sze, N. D., and Weisenstein, D. K.: Increase in levels of stratospheric chlorine and fluorine loading between 1985 and 1992, *Geophys. Res. Lett.*, 21, 2223–2226, 1994.
- Gunson, M. R., Abbas, M. M., Abrams, M. C., Allen, M., Brown, L. R., Brown, T. L., Chang, A. Y., Goldman, A., Irion, F. W., Lowes, L. L., Mahieu, E., Manney, G. L., Michelsen, H. A., Newchurch, M. J., Rinsland, C. P., Salawitch, R. J., Stiller, G. P., Toon, G. C., Yung, Y. L., and Zander, R.: The atmospheric trace molecule spectroscopy (ATMOS) experiment: Deployment on the ATLAS Space Shuttle missions, *Geophys. Res. Lett.*, 23, 2333–2336, 1996.
- Hase, F., Hannigan, J. W., Coffey, M. T., Goldman, A., Höpfner, M., Jones, N. B., Rinsland, C. P., and Wood, S. W.: Intercomparison of retrieval codes used for the analysis of high-resolution, ground-based FTIR measurements, *J. Quant. Spectros. Radiat. Transfer*, 87, 25–52, 2004.
- Hauchecorne, A., Godin, S., Marchand, M., Heese, B., and Souprayen, C.: Quantification of the transport of chemical constituents from the polar vortex to midlatitudes in the lower stratosphere using the high-resolution advection model MIMOSA and effective diffusivity, *J. Geophys. Res.*, 107(D20), 8289, doi:10.1029/2001JD000491, 2002.

- Hoppel, K. W., Bowman, K. P., and Bevilacqua, R. M.: Northern hemisphere summer ozone variability observed by POAM II, *Geophys. Res. Lett.*, 26, 827–830, 1999.
- Johnson, D. G., Jucks, K. W., Traub, W. A., and Chance, K. V.: Smithsonian stratospheric far-infrared spectrometer and data reduction system, *J. Geophys. Res.*, 100(D2), 3091–3106, doi:10.1029/94JD02685, 1995.
- Jucks, K. W., Johnson, D. G., Chance, K. V., Traub, W. A., Margitan, J. M., Stachnik, R., Sasano, Y., Yokota, T., Kanzawa, H., Shibasaki, K., Suzuki, M., and Ogawa, T. S.: Validation of ILAS v5.2 data with FIRS-2 balloon observations, *J. Geophys. Res.*, 107(D24), 8207, doi:10.1029/2001JD000578, 2002.
- Kagawa, A., Kasai, Y., Jones, N. B., Yamamori, M., Seki, K., Murcray, F., Murayama, Y., Mizutani, K., and Itabe, T.: Characteristics and error estimation of stratospheric ozone and ozone-related species over Poker Flat (65° N, 147° W), Alaska observed by a ground-based FTIR spectrometer from 2001 to 2003, *Atmos. Chem. Phys.*, 7, 3791–3810, 2007, <http://www.atmos-chem-phys.net/7/3791/2007/>.
- Kaye, J. A., Douglas, A. R., Jackman, C. H., Stolarski, R. S., Zander, R., and Roland, G.: Two-dimensional model calculations of fluorine-containing reservoir species in the stratosphere, *J. Geophys. Res.*, 96, 12 865–12 881, 1991.
- Kopp, G., Berg, H., Blumenstock, T., Fischer, H., Hase, F., Hochschild, G., Höpfner, M., Kouker, W., Reddmann, T., Ruhnke, R., Raffalski, U., and Kondo, Y.: Evolution of ozone and ozone related species over Kiruna during the THESEO 2000-SOLVE campaign retrieved from ground-based millimeter wave and infrared observations, *J. Geophys. Res.*, 108(D5), 8308, doi:10.1029/2001JD001064, 2003.
- Lary, D. J., Waugh, D. W., Douglass, A. R., Stolarski, R. S., Newman, P. A., and Mussa, H.: Variations in stratospheric inorganic chlorine between 1991 and 2006, *Geophys. Res. Lett.*, 34, L21811, doi:10.1029/2007GL030053, 2007.
- Mahieu, E., Duchatelet, P., Zander, R., Demoulin, P., Servais, C., Rinsland, C. P., Chipperfield, M. P., and De Mazière, M.: The evolution of inorganic chlorine above the Jungfraujoch station: An update, in: *Ozone, Vol. II, Proceedings of the XX Quadrennial Ozone Symposium, Kos, Greece, 1–8 June 2004*, 997–998, 2004.
- Mahieu, E., Zander, R., Duchatelet, P., Hannigan, J. W., Coffey, M. T., Mikuteit, S., Hase, F., Blumenstock, T., Wiacek, A., Strong, K., Taylor, J. R., Mittermeier, R., Fast, H., Boone, C. D., McLeod, S. D., Walker, K. A., Bernath, P. F., and Rinsland, C. P.: Comparisons between ACE-FTS and ground-based measurements of stratospheric HCl and ClONO₂ loadings at northern latitudes, *Geophys. Res. Lett.*, 32, L15S08, doi:10.1029/2005GL022396, 2005.
- McElroy, C. T., Nowlan, C. R., Drummond, J. R., Bernath, P. F., Barton, D. V., Dufour, D. G., Midwinter, C., Hall, R. B., Ogyu, A., Ullberg, A., Wardle, D. I., Kar, J., Zou, J., Nichitieu, F., Boone, C. D., Walker, K. A., and Rowlands, N.: The ACE-MAESTRO Instrument on SCISAT: description, performance and preliminary results, *Appl. Opt.*, 46, 20, 4341–4356, 2007.
- McHugh, M., Magill, B., Walker, K. A., Boone, C. D., Bernath, P. F., and Russell III, J. M.: Comparison of atmospheric retrievals from ACE and HALOE, *Geophys. Res. Lett.*, 32, L15S10, doi:10.1029/2005GL022403, 2005.
- Molina, M. J. and Rowland, F. S.: Stratospheric sink for chlorofluoromethanes: chlorine atom-catalysed destruction of ozone, *Nature*, 249, 810–812, 1974.
- Montzka, S. A., Butler, J. H., Elkins, J. W., Thompson, T. M., Clarke, A. D., and Lock, L. T.: Present and future trends in the atmospheric burden of ozone-depleting halogens, *Nature*, 398, 690–694, 1999.
- Moreau, G., Robert, C., Catoire, V., Chartier, M., Camy-Peyret, C., Huret, N., Pirre, M., Pomathiod, L., and Chalumeau, G.: SPIRALE: a multispecies in situ balloon-borne instrument with six tunable diode laser spectrometers, *Appl. Opt.*, 44, 28, 5972–5989, 2005.
- Murcray, D. G., Bonomo, F. S., Brooks, J. N., Goldman, A., Murcray, F. H., and Williams, W. J.: Detection of fluorocarbons in the stratosphere, *Geophys. Res. Lett.*, 2, 109–112, 1975.
- Nassar, R., Bernath, P. F., Boone, C. D., Clerbaux, C., Coheur, P. F., Dufour, G., Froidevaux, L., Mahieu, E., McConnell, J. C., McLeod, S. D., Murtagh, D. P., Rinsland, C. P., Semeniuk, K., Skelton, R., Walker, K. A., and Zander, R.: A global inventory of stratospheric chlorine in 2004, *J. Geophys. Res.*, 111, D22312, doi:10.1029/2006JD007073, 2006a.
- Nassar, R., Bernath, P. F., Boone, C. D., McLeod, S. D., Skelton, R., Walker, K. A., Rinsland, C. P., and Duchatelet, P.: A global inventory of stratospheric fluorine in 2004 based on Atmospheric Chemistry Experiment Fourier Transform Spectrometer (ACE-FTS) measurements, *J. Geophys. Res.*, 111, D22313, doi:10.1029/2006JD007395, 2006b.
- Notholt, J., Toon, G. C., Sen, B., Jones, N. B., Rinsland, C. P., Lehmann, R., and Rex, M.: Variations in the tropical uplift following the Pinatubo eruption studied by infrared solar absorption spectrometry, *Geophys. Res. Lett.*, 27, 2609–2612, 2000.
- O'Doherty, S., Cunnold, D. M., Manning, A., Miller, B. R., Wang, R. H. J., Krummel, P. B., Fraser, P. J., Simmonds, P. G., McCulloch, A., Weiss, R. F., Salameh, P., Porter, L. W., Prinn, R. G., Huang, J., Sturrock, G., Ryall, D., Derwent, R. G., and Montzka, S. A.: Rapid growth of HFC-134a, HCFC-141b, HCFC-142b and HCFC-22 from AGAGE observations at Cape Grim, Tasmania and Mace Head, Ireland, *J. Geophys. Res.*, 109(D6), D06310, doi:10.1029/2003JD004277, 2004.
- Paton-Walsh, C., Jones, N. B., Wilson, S. R., Haverd, V., Meier, A., Griffith, D. W. T., and Rinsland, C. P.: Measurements of trace gas emissions from Australian forest fires and correlations with coincident measurements of aerosol optical depth, *J. Geophys. Res.*, 110, D24305, doi:10.1029/2005JD006202, 2005.
- Prinn, R. G., Zander, R., Elkins, J. W., Fraser, P. J., Ko, M. K. W., Cunnold, D., Engel, A., Gunson, M. R., Mahieu, E., Midgley, P. M., Russell III, J. M., and Weiss, R. F.: Long-lived ozone-related compounds, Scientific Assessment of Ozone Depletion: 1998, WMO Report No. 44, I-1 to I-54, World Meteorological Organization, P.O. Box 2300, Geneva 2, CH 1211, Switzerland, ISBN 92-807-1722-7, 1999.
- Raper, O. F., Farmer, C. B., Zander, R., and Park, J. H.: Infrared spectroscopic measurements of halogenated sink and reservoir gases in the stratosphere with the ATMOS instrument, *J. Geophys. Res.*, 92, 9851–9858, 1987.
- Reber, C. A., Trevathan, C. E., McNeal, R. J., and Luther, M. R.: The Upper Atmosphere Research Satellite (UARS) Mission, *J. Geophys. Res.*, 98, 10 643–10 647, 1993.
- Rinsland, C. P., Zander, R., Mahieu, E., Chiou, L. S., Goldman, A., and Jones, N. B.: Stratospheric HF column abundances above

- Kitt Peak (31.9° N latitude): Trends from 1977 to 2001 and correlations with stratospheric HCl columns, *J. Quant. Spectrosc. Radiat. Transfer*, 74, 205–216, 2002.
- Rinsland, C. P., Mahieu, E., Zander, R., Jones, N.B., Chipperfield, M. P., Goldman, A., Anderson, J., Russell III, J. M., Demoulin, P., Notholt, J., Toon, G. C., Blavier, J.-F., Sen, B., Sussmann, R., Wood, S. W., Meier, A., Griffith, D. W. T., Chiou, L. S., Murcray, F. J., Stephen, T. M., Hase, F., Mikuteit, S., Schulz, A., and Blumenstock, T.: Long-term trends of inorganic chlorine from ground-based infrared solar spectra: Past increases and evidence for stabilization, *J. Geophys. Res.*, 108(D8), 4252, ACH10, doi:10.1029/2002JD003001, 2003.
- Rinsland, C. P., Goldman, A., Mahieu, E., Zander, R., Chiou, L. S., Hannigan, J. W., Wood, S. W., and Elkins, J. W.: Long-term evolution in the tropospheric concentration of chlorofluorocarbon 12 (CCl₂F₂) derived from high-spectral resolution infrared solar absorption spectra: retrieval and comparison with in situ surface measurements, *J. Quant. Spectrosc. Radiat. Transfer*, 92, 201–209, 2005.
- Rodgers, C. D.: Retrieval of atmospheric temperature and composition from remote measurements of thermal radiation, *Rev. Geophys. Sp. Phys.*, 14, 609–624, 1976.
- Rodgers, C. D. and Connor, B. J.: Intercomparison of remote sounding instruments, *J. Geophys. Res.*, 108, 4116–4129, 2003.
- Rothman, L. S., Jacquemart, D., Barbe, A., Chris Benner, D., Birk, M., Brown, L. R., Carleer, M. R., Chackerian Jr., C., Chance, K., Coudert, L. H., Dana, V., Devi, V. M., Flaud, J.-M., 30 Gamache, R. R., Goldman, A., Hartmann, J.-M., Jucks, K. W., Maki, A. G., Mandin, J.-Y., Massie, S. T., Orphal, J., Perrin, A., Rinsland, C. P., Smith, M. A. H., Tennyson, J., Tolchenov, R. N., Toth, R. A., Vander Auwera, J., Varanasi, P., and Wagner, G.: The HITRAN 2004 molecular spectroscopic database, *J. Quant. Spect. Rad. Trans.*, 96, 139–204, 2005.
- Russell III, J. M., Gordley, L. L., Park, J. H., Drayson, S. R., Hesketh, D. H., Cicerone, R. J., Tuck, A. F., Frederick, J. E., Harries, J. E., and Crutzen, P. J.: The Halogen Occultation Experiment, *J. Geophys. Res.*, 98, 10 777–10 797, 1993.
- Russell III, J. M., Deaver, L. E., Luo, M., et al.: Validation of hydrogen chloride measurements made by the Halogen Occultation Experiment from the UARS platform, *J. Geophys. Res.*, 101(D6), 10 151–10 162, 1996a.
- Russell III, J. M., Deaver, L. E., Luo, M., et al.: Validation of hydrogen fluoride measurements made by the Halogen Occultation Experiment from the UARS platform, *J. Geophys. Res.*, 101(D6), 10 163–10 174, 1996b.
- Schneider, M., Blumenstock, T., Chipperfield, M. P., Hase, F., Kouker, W., Reddmann, T., Ruhnke, R., Cuevas, E., and Fischer, H.: Subtropical trace gas profiles determined by ground-based FTIR spectroscopy at Izaña (28° N, 16° W): Five-year record, error analysis, and comparison with 3-D CTMs, *Atmos. Chem. Phys.*, 5, 153–167, 2005, <http://www.atmos-chem-phys.net/5/153/2005/>.
- Sen, B., Toon, G. C., Osterman, G. B., Blavier, J.-F., Margitan, J. J., Salawitch, R. J., and Yue, G. K.: Measurements of reactive nitrogen in the stratosphere, *J. Geophys. Res.*, 103(D3), 3571–3585, doi:10.1029/97JD02468, 1998.
- Senten, C., De Mazière, M., Dils, B., Hermans, C., Kruglanski, M., Neefs, E., Scolas, F., Vandaele, A. C., Vanhaelewyn, G., Vigouroux, C., Carleer, M., Coheur, P. F., Fally, S., Barret, B., Baray, J. L., Delmas, R., Leveau, J., Metzger, J. M., Mahieu, E., Boone, C., Walker, K. A., Bernath, P. F., and Strong, K.: Technical Note: New ground-based FTIR measurements at Ile de La Réunion: observations, error analysis, and comparisons with independent data, *Atmos. Chem. Phys.*, 8, 3483–3508, 2008, <http://www.atmos-chem-phys.net/8/3483/2008/>.
- Solomon, S.: Stratospheric ozone depletion: a review of concepts and history, *Rev. Geophys.*, 37, 275–316, 1999.
- Stolarski, R. S. and Rundel, R. D.: Fluorine photochemistry in the stratosphere, *Geophys. Res. Lett.*, 2, 443–444, 1975.
- Toon, G. C.: The JPL MkIV interferometer, *Opt. Photonics News*, 2, 19–21, 1991.
- Toon, G. C., Blavier, J.-F., Sen, B., Margitan, J. J., Webster, C. R., May, R. D., Fahey, D. W., Gao, R., Del Negro, L., Proffitt, M., Elkins, J., Romashkin, P. A., Hurst, D. F., Oltmans, S., Atlas, E., Schauffler, S., Flocke, F., Bui, T. B., Stimpfle, R. M., Bonne, G. P., Voss, P. B., and Cohen, R. C.: Comparison of MkIV balloon and ER-2 aircraft measurements of atmospheric trace gases, *J. Geophys. Res.*, 104(D21), 26 779–26 790, doi:10.1029/1999JD900379, 1999.
- Toon, G. C., Sen, B., Osterman, G. B., Blavier, J.-F., Sasano, Y., Yokota, T., Kanzawa, H., Ogawa, T., Suzuki, M., and Shibasaki, K.: Comparison of ILAS and MkIV profiles of atmospheric trace gases measured above Alaska in May 1997, *J. Geophys. Res.*, 107(D24), 8211, doi:10.1029/2001JD000640, 2002.
- Vigouroux, C., De Mazière, M., Errera, Q., Chabrillat, S., Mahieu, E., Duchatelet, P., Wood, S., Smale, D., Mikuteit, S., Blumenstock, T., Hase, F., and Jones, N.: Comparisons between ground-based FTIR and MIPAS N₂O and HNO₃ profiles before and after assimilation in BASCOE, *Atmos. Chem. Phys.*, 7, 377–396, 2007, <http://www.atmos-chem-phys.net/7/377/2007/>.
- Waters, J. W., Froidevaux, L., Harwood, R. S., et al.: The Earth Observing System Microwave Limb Sounder (EOS MLS) on the Aura satellite, Experiment, *IEEE Trans. Geosci. Remote Sensing*, 44, 5, 1075–1092, 2006.
- Wiacek, A., Taylor, J. R., Strong, K., Saari, R., Kerzenmacher, T., Jones, N. B., and Griffith, D. W. T.: Ground-Based solar absorption FTIR spectroscopy: characterization of retrievals and first results from a novel optical design instrument at a New NDACC Complementary Station, *J. Atmos. Oceanic Technol.*, 24(3), 432–448, 2007.
- WMO Report No. 50. Scientific Assessment of Ozone Depletion: 2006. World Meteorological Organization, P.O. Box 2300, Geneva 2, CH 1211, Switzerland, 2007.
- Zander, R.: Présence de HF dans la stratosphère supérieure, *C. R. Acad. Sc. Paris*, 281b, 213–214, 1975.
- Zander, R., Rinsland, C. P., Farmer, C. B., and Norton, R. H.: Infrared spectroscopic measurements of halogenated source gases in the stratosphere with the ATMOS instrument, *J. Geophys. Res.*, 92, 9836–9850, 1987.
- Zander, R., Gunson, M. R., Farmer, C. B., Rinsland, C. P., Irion, F. W., and Mahieu, E.: The 1985 chlorine and fluorine inventories in the stratosphere based on ATMOS observations at 30° north latitudes, *J. Atmos. Chem.*, 15, 171–186, 1992.
- Zander, R., Mahieu, E., Gunson, M. R., Abrams, M. C., Chang, A. Y., Abbas, M., Aellig, C., Engel, A., Goldman, A., Irion, F. W., Kämpfer, N., Michelsen, H. A., Newchurch, M. J., Rinsland, C. P., Salawitch, R. J., Stiller, G. P., and Toon, G. C.: The

- 1994 northern midlatitude budget of stratospheric chlorine derived from ATMOS/ATLAS-3 observations, *Geophys. Res. Lett.*, 23, 2357–2360, 1996.
- Zander, R., Mahieu, E., Demoulin, P., Duchatelet, P., Servais, C., Roland, G., Delbouille, L., De Mazière, M., and Rinsland, C. P.: Evolution of a dozen non-CO₂ greenhouse gases above Central Europe since the mid-1980s, *Environ. Sci.*, 2(2–3), 295–303, 2005.
- Zander, R., Mahieu, E., Demoulin, P., Duchatelet, P., Roland, G., Servais, C., De Mazière, M., Reimann, S., and Rinsland, C. P.: Our changing atmosphere: evidence based on long-term infrared solar observations at the Jungfraujoch since 1950, *Sci. Total Environ.*, 391, 184–195, 2008.